*Published online 27 February 2018*

*Nucleic Acids Research, 2018, Vol. 46, No. 9* ***4487–4504***
*doi: 10.1093/nar/gky155*

# ATF7 mediates TNF-α–induced telomere shortening

**Toshio Maekawa[1,†], Binbin Liu[1,2,†], Daisuke Nakai[1,2], Keisuke Yoshida[1], Ken-ichi Nakamura[3], Mami Yasukawa[4], Manabu Koike[5], Kaiyo Takubo[3], Bruno Chatton[6], Fuyuki Ishikawa[7], Kenkichi Masutomi[4] and Shunsuke Ishii[1,2,*]**

[1]Laboratory of Molecular Genetics, RIKEN Tsukuba Institute, 3-1-1 Koyadai, Tsukuba, Ibaraki 305-0074, Japan, [2]Graduate School of Comprehensive Human Sciences, University of Tsukuba, 1-1-1 Tennoudai, Tsukuba, Ibaraki 305-8577, Japan, [3]Research Team for Geriatric Diseases, Tokyo Metropolitan Institute of Gerontology, Sakaecho 35-2, Itabashi-ku, Tokyo 173-0015, Japan, [4]Division of Cancer Stem Cell, National Cancer Center Research Institute, Tokyo, Japan, [5]National Institute of Radiological Sciences, National Institutes for Quantum and Radiological Science and Technology, 4-9-1 Anagawa, Inage-ku, Chiba 263-8555, Japan, [6]Université de Strasbourg, UMR7242 Biotechnologie et Signalisation Cellulaire, Ecole Supérieure de Biotechnologie de Strasbourg, BP10413, Illkirch, France and [7]Department of Gene Mechanisms, Graduate School of Biostudies, Kyoto University, Yoshida-Konoe-cho, Sakyo-ku, Kyoto 606-8501, Japan

Received August 29, 2017; Revised February 13, 2018; Editorial Decision February 13, 2018; Accepted February 20, 2018

## ABSTRACT

**Telomeres maintain the integrity of chromosome ends and telomere length is an important marker of aging. The epidemiological studies suggested that many types of stress including psychosocial stress decrease telomere length. However, it remains unknown how various stresses induce telomere shortening. Here, we report that the stress-responsive transcription factor ATF7 mediates TNF-α–induced telomere shortening. ATF7 and telomerase, an enzyme that elongates telomeres, are localized on telomeres via interactions with the Ku complex. In response to TNF-α, which is induced by various stresses including psychological stress, ATF7 was phosphorylated by p38, leading to the release of ATF7 and telomerase from telomeres. Thus, a decrease of ATF7 and telomerase on telomeres in response to stress causes telomere shortening, as observed in ATF7-deficient mice. These findings give credence to the idea that various types of stress might shorten telomere.**

## INTRODUCTION

Telomeres, which consist of tandem TTAGGG repeats and are associated shelterin multi-protein complex, maintain the integrity of chromosome ends during cell division (1,2). In most somatic cells, telomere length shortens with each cell division and is therefore an important marker of aging (3). Telomeres can be elongated enzymatically by telomerase, a complex consisting of a catalytic subunit (TERT) and an RNA subunit, which counterbalances the effects of cell division (1,2,4). Telomere shortening and telomerase mutations are associated with various human diseases, such as cancers and dyskeratosis congenita (5), as well as changes in cellular metabolism (6). Several types of stress decrease telomere length: exposure to psychosocial stress is associated with telomere shortening (7); prenatal stress exposure causes shorter telomere length later in life (8); and oxidative stress shortens telomeres (9). However, it remains unknown how various stresses induce telomere shortening.

In the yeast *Saccharomyces cerevisiae*, the Ku complex, a heterodimer of Ku70 and Ku80 subunits, directly interacts with the telomerase RNA subunit TLC1 (10), which affects the association of TERT (Est2 in yeast) with telomeres when they are normally elongated in late S/G2 phase (11). Furthermore, yeast Ku loads onto telomeres (12), and it was shown that Ku recruits telomerase to telomere in *S. cerevisiae* (13). On the other hand, the role of Ku in the regulation of telomere length has not been demonstrated as clearly in vertebrates as in yeast. Human Ku is associated with human TERT (hTERT) (14) and telomeres (15), and conditional loss of human Ku80 causes massive telomere loss in the human cell line HCT116 (16). However, conflicting results have been published regarding telomere shortening in *Ku70* or *Ku80* knockout mice. Telomere shortening in *Ku70*- or *Ku80*-deficient cells was observed by one group (17), but another group observed no telomere shortening in *Ku80*-deficient MEFs (18). Thus, the role of Ku in the regulation of telomere length in mammals remains unclear.

We speculated that ATF7, a stress-responsive chromatin regulator, could be involved in stress-induced telomere shortening. ATF7 is a vertebrate member of the ATF2

*To whom correspondence should be addressed. Tel: +81 29 836 9031; Fax: +81 29 836 9030; E-mail: sishii@rtc.riken.jp
†These authors contributed equally to this work as first authors.

subfamily of transcription factors, which belong to the ATF/CREB superfamily of proteins; these proteins are characterized by the presence of B-Zip DNA-binding domains (19–21). The ATF2 proteins are phosphorylated by p38 in response to environmental, oxidative, psychological, and nutritional stress, as well as pathogen infection (22,23). In the absence of stress, ATF7 silences transcription of target genes, such as the gene encoding serotonin receptor 5b, by recruiting the ESET/SET-DB1 histone H3K9 trimethyltransferase to promote formation of a heterochromatin-like structure (24,25). Social isolation, a kind of psychological stress, can induce ATF7 phosphorylation by p38 in the brain, possibly by elevating the levels of inflammatory cytokines (e.g., TNF-α) in the periphery (24). ATF7 phosphorylation causes release of ATF7 and ESET from their target genes, leading to transcriptional activation. In mouse macrophages, ATF7 also silences a group of genes involved in innate immunity by recruiting the histone H3K9 dimethyltransferase G9a (26). Pathogen infection induces ATF7 phosphorylation via the Toll-like receptors (TLRs)/p38 pathway and releases ATF7-G9a from target genes, leading to transcriptional activation and long-term maintenance of the higher basal expression levels. *Drosophila* ATF2 (dATF2) and yeast *Schizosaccharomyces pombe* Atf1 are orthologs of ATF7, and both of these proteins contribute to heterochromatin formation (27,28). Environmental stresses, such as heat shock or osmotic stress, induce dATF2 phosphorylation and cause release of dATF2 from heterochromatic structures, leading to an inheritable disruption of heterochromatin (27).

Recently, we found that *in utero* TNF-α treatment induces telomere shortening in various tissues of adult mice in the ATF7-dependent manner (29). Here, we have further analyzed the mechanism of TNF-α-induced and ATF7-dependent telomere shortening. Loss of ATF7 shortens telomere length in mice and that ATF7 and telomerase are localized on telomere via binding to the Ku complex. Furthermore, TNF-α treatment induces a release of ATF7 and telomerase through ATF7 phosphorylation by p38, resulting in telomere shortening.

## MATERIALS AND METHODS

### Mice

Mice were maintained under specific pathogen-free conditions on a 12 h light–dark cycle and fed a normal diet (CE-2 from CLEA Inc., composed of 12 kcal% fat, 29 kcal% protein and 59 kcal% carbohydrates) (Nestle Purina). Congenic *Atf7*$^{-/-}$, *Tert*$^{-/-}$, and *Ku70*$^{-/-}$ mice in the C57BL/6 genetic background were described previously (24,30,31). Experiments were conducted in accordance with the guidelines of the Institutional Animal Care and Use Committee of the RIKEN Tsukuba Branch and the National Institute of Radiological Sciences.

### Preparation of MEFs

Mouse embryonic fibroblasts (MEFs) were prepared from E14.5 embryos from WT and G2 *Atf7*$^{-/-}$ mice in the C57BL/6 genetic background. TNF-α (20 μg/kg weight) was intraperitoneally administered to pregnant mice daily from E2.5 to E14.5. Congenic *Tert*$^{-/-}$ mice in the C57BL/6 genetic background (30) were interbred, and MEFs were prepared from E14.5 embryos from G4 *Tert*$^{-/-}$ mice. Congenic *Ku70*$^{+/-}$ mice in the C57BL/6 genetic background (31) were interbred, and WT and *Ku70*$^{-/-}$ MEFs were prepared from E14.5 embryos.

### Cells, ATF7 or Ku70 knockdown, and TNF-α treatment

MEFs, HeLa S3 cells, and *Ku70*$^{-/-}$ mouse lung epithelial (MLE) cells (32) were used. ATF7 or Ku70 knockdown was performed using siRNA or lentivirus expressing shRNA (Supplementary Table S1). For telomere length analysis, HeLa cells were cultured for a further 14 days with or without daily TNF-α (100 ng/ml) treatment after knockdown of ATF7 or Ku70.

### Metaphase analysis to detect end-to-end fusion

MEFs were treated as Q-FISH and stained with modified giemsa stain solution GS500 (Sigma).

### Measurement of telomere length

Telomere length of MEFs and HeLa cells were was analyzed by Q-FISH, real-time PCR, and TRF (Telomere Restriction Fragment) assay. Q-FISH and image analysis were performed as described previously (33,34). A real-time quantitative PCR method previously described (35,36) was used. TRF (Telomere Restriction Fragment) assay was performed using the standard assay using $^{32}$P-labeled oligonucleotide telomeric probes (Supplementary Table S1).

### ATF7 complex purification

The complex was purified essentially as described previously (37). Nuclear extracts were prepared from HeLa S3 cell clone expressing Flag/HA-tagged ATF7, and the ATF7 complexes were immunopurified using anti-Flag and anti-HA antibodies. The purified proteins were analyzed by mass spectrometry.

### Analysis of phosphorylation of ATF7 and p38 in response to TNF-α

After media on HeLa S3 cell cultures was replaced with fresh medium, the p38 inhibitor SB203580 (20 μM) was added. Two hours later, the cells were treated with TNF-α (100 ng/ml) for the indicated period. Cells were washed with cold PBS three times, and nuclear extracts were prepared according to the Dignam method (38). ATF7 and p38 were detected by western blotting using anti-ATF7 (1A7), anti-pATF7 (#9225, CST), anti-p38 (#9212, CST), anti-phospho-p38 (#9211, CST),

### Identification of endogenous human TERT

We (Masutomi and colleagues) generated a series of anti-hTERT monoclonal antibodies (mAb) by immunizing mice with a recombinant truncated version of hTERT (amino acids 304–460), and two of them (mAb 10E9-2 and 2E4-2)

were used in this study. Validation of the specificity of mAb 10E9-2 for immunoprecipitation was previously described (39). To test the specificity of mAb 2E4-2 for the western blotting, we expressed *hTERT*-specific siRNAs (40). Expression of these siRNAs eliminated the signal (Supplementary Figure S7), indicating that the signal corresponds to endogenous hTERT. HeLa S3 cells were lysed by mild sonication in 1 ml of Lysis buffer (20 mM Tris–HCl [pH 7.4], 0.5% NP-40, 150 mM NaCl, Protease Inhibitor Cocktail [Sigma]). Lysates were immunoprecipitated with anti-hTERT mAb 10E9-2 followed by addition of protein A-Sepharose (GE Healthcare). The beads were washed five times with lysis buffer. Immunocomplexes were resolved on 8% SDS polyacrylamide gels and analyzed by western blotting with anti-hTERT mAb 2E4-2 and mouse IgG TrueBlot® Ultra (Rockland). In some cases, HeLa S3 cells were transfected with siRNA against hTERT; 5 days later, cell lysates were prepared and immuno-precipitated, followed by western blotting, as described above.

### Co-immunoprecipitation of the ATF7/Ku/TERT complex

Lysates from HeLa S3 cells stably expressing Flag-ATF7 were immunoprecipitated using anti-Flag. Immunocomplexes were analyzed by western blotting with anti-ATF7, anti-Ku70, anti-Ku80, anti-TERT monoclonal antibody 2E4-2, or anti-Suv39h1 antibodies. In the two-step co-immunoprecipitation, Flag-ATF7 complexes were first immunoprecipitated with anti-Flag. After elution with Flag peptide, the second immunoprecipitation was performed using anti-TERT monoclonal antibody 10E9-2.

### ChIP/slot-blot hybridization

After MEFs, HeLa S3 cells, or MLE cells were crosslinked, chromatin was solubilized, and DNA was sheared by sonication. Immunoprecipitation was carried out with anti-ATF7, anti-Ku70, anti-Ku80, anti-TERT mAb 10E9-2, anti-histone H3, anti-histone H3 K9me3 or anti-Suv39h1 antibodies. DNA was purified from immunocomplexes, and blotted. Hybridization was done using the $^{32}$P-labeled telomeric and Alu probes.

### Statistics

We used the Mantel−Cox log-rank test to calculate the statistical significance (*P* value) of differences between survival curves. Results of Q-PCR, qRT-PCR, TRAP assay, ChIP/slot-blot hybridization, and q-ChIP are presented as means ± standard deviation (SD). Differences between groups were examined for statistical significance using Student's *t*-test. In Q-FISH assay, Fisher's Z test was used for comparisons of relationships.

All Materials and Methods are described in detail in Supplementary Data.

## RESULTS

### Telomere shortening in ATF7-deficient mouse cells

To test whether ATF7 affects the telomere length, we compared the telomere lengths of mouse embryonic fibroblasts (MEFs) prepared from WT and G2 *Atf7*$^{-/-}$ mice. To minimize mouse-to-mouse variation, telomere length was measured in three independent MEFs obtained from three independent pregnant mice in all experiments. The results obtained using three different methods, namely, quantitative real-time PCR (Q-PCR), quantitative fluorescence *in situ* hybridization (Q-FISH), and telomere restriction fragment (TRF) analysis, indicated that telomere length was shorter in *Atf7*$^{-/-}$ MEFs than in WT MEFs (Figure 1A, C and E; Supplementary Figure S1). The Q-FISH data, which were the most reliable quantitative data, indicated that telomere fluorescence intensity (TFI) was 14.1% lower in *Atf7*$^{-/-}$ MEFs than in WT cells. Telomeres showed progressive shortening with increasing generation time in telomerase RNA mutant mice, mTR (41), while Q-PCR and Q-FISH analyses showed that there was no difference in the telomere length of MEFs of G1 (data not shown), G2 and G12 mice (Supplementary Figure S2), indicating that the generation-dependent shortening did not occur in *Atf7*$^{-/-}$ mice. This difference could be due to the maintenance of normal levels of telomerase expression in *Atf7*$^{-/-}$ mice (see Discussion).

### TNF-α–induced and ATF7-dependent telomere shortening in MEFs

To investigate the role of ATF7 in stress-induced telomere shortening, the telomere lengths of WT and *Atf7*$^{-/-}$ MEFs prepared from pregnant mice treated by daily injection of TNF-α from embryonic day (E) 2.5 to E14.5 were compared. TNF-α is induced by both psychological stress and pathogen infection (42); TNF-α in turn induces phosphorylation of p38 and ATF7 (24). We showed tat TNF-α, at the dose used, induced several TNF-α–inducible mRNAs, including *Cxcl10*, *Cxcl9*, *NF-κB p65* and *Cd14*, in the liver as reported previously (43) (Supplementary Figure S3A). The results obtained by Q-PCR, Q-FISH and TRF analyses indicated that telomeres were shorter in MEFs prepared from TNF-α–injected mice than in control (i.e. untreated) MEFs (Figure 1A, C and E; Supplementary Figure S1). TFI measured by Q-FISH was 9.3% lower in MEFs prepared from TNF-α–injected mice than in control MEFs. However, such TNF-α–induced decrease was not observed in *Atf7*$^{-/-}$ MEFs; in fact, telomeres were longer rather than shorter in TNF-α–treated *Atf7*$^{-/-}$MEFs than in untreated controls of the same genotype. MEFs from *Tert*$^{-/-}$ mice were used as a control. Telomere length analysis using three different methods indicated that MEFs from fourth-generation *Tert*$^{-/-}$ mice had shorter telomeres than WT MEFs, and TNF-α did not affect telomere length in *Tert*$^{-/-}$ MEFs (Figure 1B, D and F; Supplementary Figure S3B-E). This suggested that TNF-α–induced telomere shortening is telomerase-dependent.

Loss of telomerase RNA in mice is associated with an increase in the frequency of chromosomal fusions and the lack of detectable TTAGGG signal on some chromosomes (44,45). We have also examined whether *Atf7*$^{-/-}$ MEFs exhibit similar abnormalities. The frequency of chromosomal fusions in *Atf7*$^{-/-}$ MEFs (0.64 per metaphase) was 2.7-fold higher than that in WT MEFs (Figure 2). In addition, no TTAGGG signal was detected on 1.57% of the chromosomes from *Atf7*$^{-/-}$ MEFs, which is 4.9-fold higher fre-

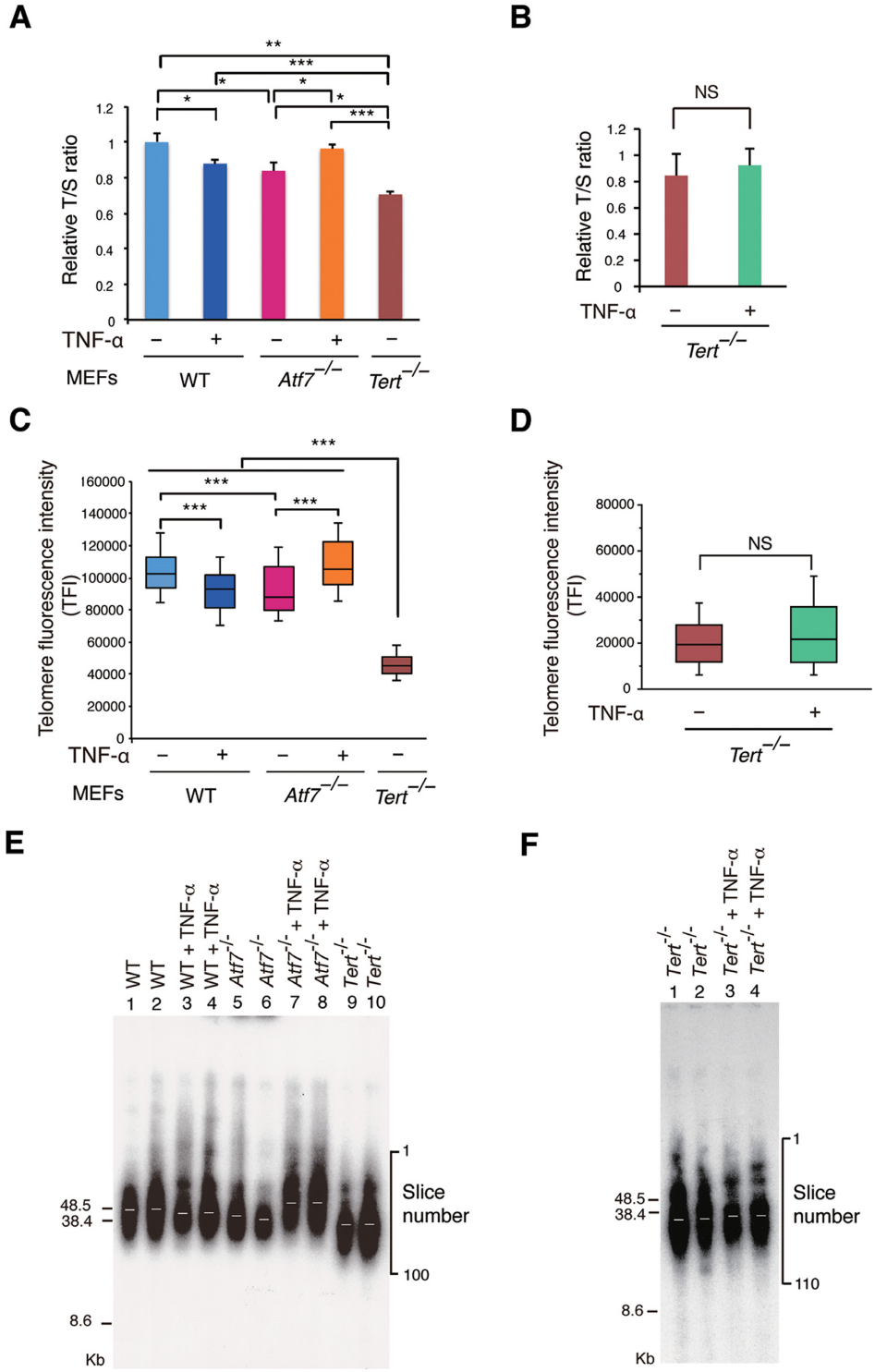


**Figure 1.** ATF7 is required for TNF-α–induced telomere shortening in MEFs. Telomere length of WT, *Atf7*$^{-/-}$ or *Tert*$^{-/-}$ MEFs prepared from TNF-α–treated or non-treated pregnant mice were analyzed by Q-PCR (A, B), Q-FISH (C, D), or telomere restriction fragment (TRF) assay using the G24 probe (E, F). MEFs from G2 *Atf7*$^{-/-}$ mice and G4 *Tert*$^{-/-}$ mice were used. Three primary MEFs from independent pregnant mice were used. (**A**, **B**) Average T/S ratio is shown ± SD. * < 0.05; **$P < 0.01$; ***$P < 0.001$; NS, not significant. See Supplementary Figure S1A, B for control data. (**C**, **D**) Middle lines in the colored boxes indicate medians; top and bottom edges, 25th and 75th percentiles; and whiskers, 10th and 90th percentiles. Note that data in Figure 2C and D cannot be directly compared because those experiments were separately performed. See Supplementary Figure S1C, D for raw data. (**E**, **F**) In TRF assays performed using mouse samples, the fragment detected was relatively long, and determination of the precise size was difficult. Therefore, the radioactivity of each slice in each lane (slice number is shown on the right) was quantitated using Image Analyzer, and the position of mean radioactivity was calculated. White bars indicate the position (slice number) of mean radioactivity in various samples: E, lanes 1–10; 47.2, 46.4, 49.6, 49.5, 52.0, 54.6, 42.0, 41.6, 58.7 and 57.7, respectively; F, lanes 1–4; 61.9, 61.3, 58.8 and 58.4, respectively. Note that we determined the position of mean length here, because the mouse telomere size is big and hard to determine precisely, and also the purpose of this experiment is the comparison of telomere size.

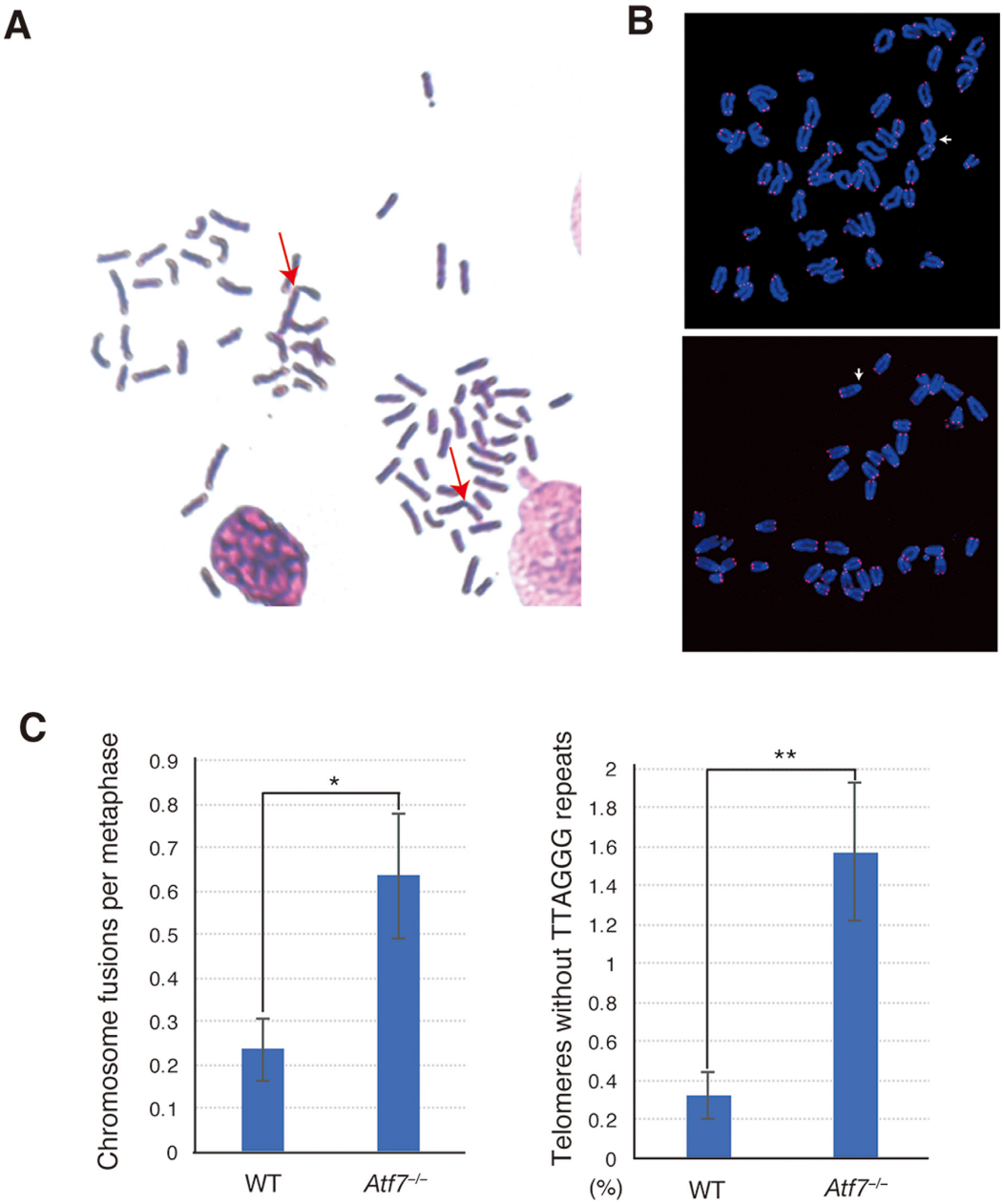


**Figure 2.** Loss of ATF7 increases the frequency of chromosomal fusions and the lack of detectable TTAGGG signal at the chromosome ends. (**A**) Metaphase spreads derived from *Atf7*$^{-/-}$ MEFs were examined for abnormal chromosome number. Arrows indicate the chromosomal fusion. (**B**) Telomere FISH images of *Atf7*$^{-/-}$ MEFs are shown. White arrows indicate the chromosomes which lack fluorescence signal at the chromosome end. (**C**) Summary of cytogenetic observations and quantitative FISH data in WT and *Atf7*$^{-/-}$MEFs. The frequency of chromosomal fusions and the lack of detectable TTAGGG signal were examined using three independent WT and *Atf7*$^{-/-}$ MEFs obtained from three independent pregnant mice. The number of the metaphase analyzed was 25, 22 and 20 (total 67) for WT MEFs, while 15, 15 and 14 (total 44) for *Atf7*$^{-/-}$ MEFs. Average value is shown ± SD. *$P < 0.05$; **$P < 0.01$.

quency compared to that in WT cells (Figure 2). The associated appearance of chromosomal fusions and the loss of telomere signal indicate that the loss of ATF7 leads to telomere shortening and chromosome instability.

The TNF-α–induced telomere lengthening was observed only in *Atf7*$^{-/-}$MEFs, but not in WT cells. We have analyzed this mechanism. Because it was reported that TNF-α promotes nuclear import of TERT together with NF-κB-p65 (46), TNF-α–induced telomere lengthening in *Atf7*$^{-/-}$MEFs might have resulted from increased levels of TERT in the nucleus. To test this, using the HA-tagged TERT expression vector (47), TERT and NF-κB-p65 levels were measured in nuclear and cytosolic fractions from MEFs treated with TNF-α with HeLa cells as the control. In MEFs, the nuclear translocation of both TERT and NF-κB-p65 increased at 1 h after the addition of TNF-α, and this increase was maintained at 2 h after TNF-α addition (Supplementary Figure S4A). However, in HeLa cells, nu-

clear translocation of TERT was only slightly induced at 1 h after the addition of TNF-α, and this induction was not maintained at 2 h after TNF-α addition. These results indicated that the enhancement of nuclear entry of TERT induced by TNF-α treatment was more evident in MEFs than in HeLa cells. Thus, in HeLa cells, TNF-α-induced telomere lengthening, which might be caused by the TNF-α-induced nuclear entry of TERT, may not be observed (see below). The molecular mechanism underlying the different degree of TNF-α-induced nuclear transfer of NF-κB-p65 between MEFs and HeLa cells is unknown at present. However, increasing evidences indicated that the TNF-α responsiveness varies among different cell types, which depends mainly on the signaling pathway downstream of the TNF-α receptor. For instance, it was shown that the level of IKKγ/NEMOΔ is much higher in HeLa S3 cells compared to that in MEFs (48). IKKγ/NEMOΔ binds to both IKK-α and β, and inhibits the TNF-α-induced NF-κB activation as a dominant-negative form. Such difference may explain the weaker TNF-α responsiveness of HeLa S3 cells compared to MEFs.

### TNF-α–induced and ATF7-dependent telomere shortening in HeLa cells

To test whether ATF7 also mediates TNF-α–induced telomere shortening in human cells, we used HeLa cells, in which the nuclear translocation of TERT induced by TNF-α treatment was not evident. ATF7 in HeLa cells was knocked down using siRNA (Figure 3A) or lentivirus expressing shRNA (Supplementary Figure S4B), and telomere length was measured by Q-PCR, Q-FISH, and TRF after culture for 14 days with daily TNF-α treatment. Similar results were obtained using the three different methods, and TNF-α induced telomere shortening in control HeLa cells but not in ATF7-knockdown cells (Figure 3B–D and Supplementary Figure S5A–D). Unlike in the case of *Atf7*$^{-/-}$MEFs, no telomere lengthening was induced by TNF-α in ATF7–knockdown HeLa cells, which is consistent with the observation that an enhancement of the nuclear translocation of TERT induced by TNF-α treatment was not evident in HeLa cells (Supplementary Figure S4A). After multiple passages, HeLa cells showed telomere shortening in ATF7-knockdown but not in control cells (Figure 3E and Supplementary Figure S5E and F).

### Association of ATF7 with Ku70/80 and TERT

ATF7 recognizes the cAMP response element (CRE: 5′-TGACGTCA-3′), which is not localized at telomere repeats. Our RNA expression data obtained in WT and *Atf7*$^{-/-}$ mice indicated that ATF7 does not regulate the transcription of genes involved in the regulation of telomere length (24,26). To investigate a possible mechanism underlying the TNF-α–induced and ATF7-dependent telomere shortening, we first tested whether ATF7 regulates telomerase activity. Analysis of telomerase activity using the TRAP (Telomeric Repeat Amplification Protocol) assay in extracts from normal, ATF7-knockdown, and ATF7-overexpressing HeLa cells showed no differences between the different cell types (Supplementary Figure S6A). We then examined whether TNF-α treatment induces replication fork stalling by modulating heterochromatin structure via ATF7, resulting in telomere shortening. TNF-α treatment did not induce ATR phosphorylation, a hallmark of replication fork stalling (49) (Supplementary Figure S6B). This indicated that the effect of TNF-α treatment on telomere shortening was not mediated by the induction of replication fork stalling.

To understand how ATF7 regulates telomere length in particular, we purified the ATF7 complex by two-step immuno-purification, using anti-Flag and anti-HA antibodies, from nuclear extracts prepared from HeLa cells expressing Flag/HA-tagged ATF7. Mass-spectrometric analysis of the purified ATF7 complex revealed that it contained two subunits of the Ku complex, Ku70 and Ku80 (Figure 4A). Since human Ku is associated with TERT (14) and telomeres (15), we examined the interaction of ATF7, Ku complex and TERT by two-step co-immunoprecipitation. When lysates of HeLa cells expressing Flag-ATF7 were immunoprecipitated with anti-Flag-antibody, Ku70, Ku80 and TERT were co-immunoprecipitated with Flag-ATF7 (Figure 4B, left). The immune-complexes were released by Flag peptide, and immunoprecipitated with anti-hTERT monoclonal antibody (mAb) 10E9-2 (39). We tested whether the anti-hTERT mAbs 10E9-2 can really immunoprecipitate endogenous TERT in HeLa cells. A 130 kD band was detected by immunoprecipitation of HeLa cell lysate with anti-hTERT mAb 10E9-2 followed by immunoblotting with anti-hTERT mAb 2E4-2, and this band was disappeared following expression of two kinds of siRNA against hTERT (Supplementary Figure S7), indicating that it corresponds to endogenous hTERT. Two subunits of Ku complex and Flag-ATF7 were co-immunoprecipitated with TERT (Figure 4B, right). These results demonstrated that ATF7, Ku70/80 and TERT form a complex (Figure 4B).

Ku70 and Ku80 are abundant proteins (50) and are frequently contaminants during purification. Therefore, we carefully tested whether the observed interaction between Ku proteins and ATF7 was specific. When co-immunoprecipitation using anti-Flag antibody was performed using HeLa cells expressing Flag-Ski corepressor under the same conditions of two-step co-immunoprecipitation described above, Ku70/80 were not co-immunoprecipitated (Supplementary Figure S8A), supporting the idea that ATF7 interacts specifically with the Ku complex. In addition, we used GST pull-down assays to examine the ATF7-Ku interaction as described (51). The results of binding assays using GST-ATF7 and HeLa cell lysates containing endogenous Ku70 indicated that the DNA-binding B-Zip domain of ATF7 binds to Ku70 (Supplementary Figure S8B–D). To test whether ATF7 directly binds to the Ku complex, EGFP-Ku70 was overexpressed in 293T cells, immune-purified using anti-GFP antibody, and used for the GST pull-down assay. Results indicated that EGFP-Ku70 bound to GST-ATF7-b-Zip, but not to GST (Supplementary Figure S8E), indicating that the ATF7 directly interacts with the Ku complex. Furthermore, Ku70 bound to the B-Zip domain of ATF7 but not to that of CREB (Supplementary Figure S9A and B), suggesting that the Ku complex specifically interacts with the surface of DNA-binding domain of the ATF7 dimer. In addition, the

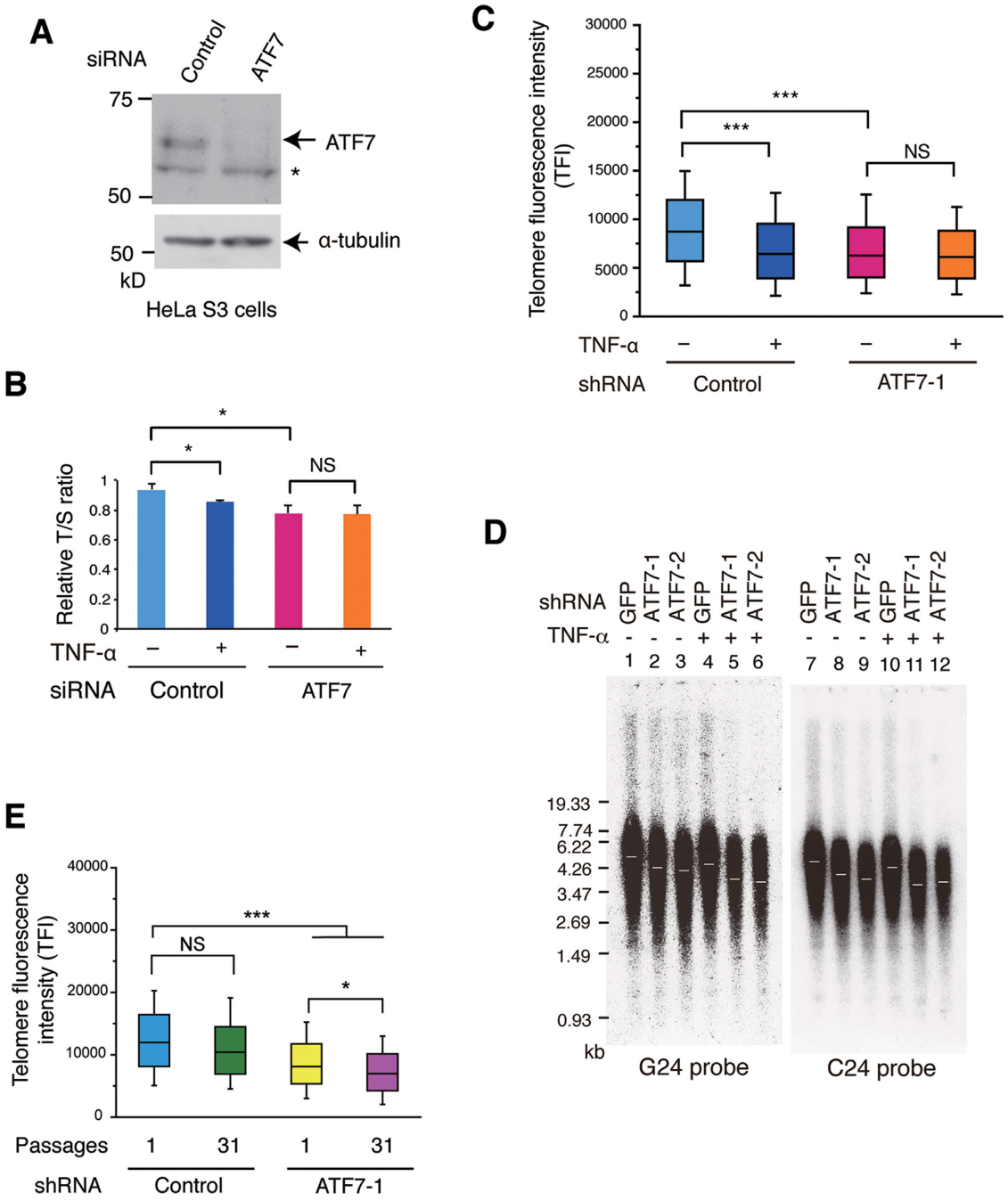


**Figure 3.** TNF-α–induced and ATF7-dependent telomere shortening in HeLa cells. (**A**) Knockdown of ATF7 in HeLa cells. HeLa cells were transfected with ATF7 siRNA, and after 72 h cell lysates were subjected to western blotting. (**B**) Telomere shortening by TNF-α in HeLa cells detected by Q-PCR. HeLa cells were transfected with ATF7 or control siRNA, and then further cultured with or without daily TNF-α treatment for 14 days. Telomere length was measured by Q-PCR, and shown as described in Figure 2A. *$P < 0.05$; NS, not significant. See Supplementary Figure S5A, B for control data. (**C**, **D**) Telomere shortening induced by TNF-α in HeLa cells was detected by Q-FISH and TRF assays. HeLa cells were infected with lentivirus expressing ATF7 or control (GFP) shRNA, and then further cultured with or without daily TNF-α treatment for 14 days. ATF7-1 and ATF7-2 correspond to different regions of ATF7 mRNA. Telomere length was measured by Q-FISH (C) or TRF assay (D). Results are shown as described in Figure 1C, E. ***$P < 0.001$; NS, not significant. See Supplementary Figure S4B for ATF7 knockdown and Supplementary Figure S5C, D for raw data of Q-FISH. White bars in (D) indicate the mean TRF length of various samples: lanes 1–12; 4.98, 4.26, 4.16, 4.5, 3.96, 3.78, 4.72, 4.01, 3.84, 4.27, 3.64 and 3.66 kb, respectively. Note that we determined the position of mean length here, because the purpose of this experiment is the comparison of telomere size. (**E**) Telomere shortening during long passage of HeLa cells. HeLa cells expressing ATF7 or control (GFP) shRNA were cultivated and passaged once or 31 times, and telomere length was analyzed by Q-FISH. Results are shown as described in Figure 2C. *$P < 0.05$; **$P < 0.01$; ***$P < 0.001$; NS, not significant. See Supplementary Figure S5E and F for raw data.

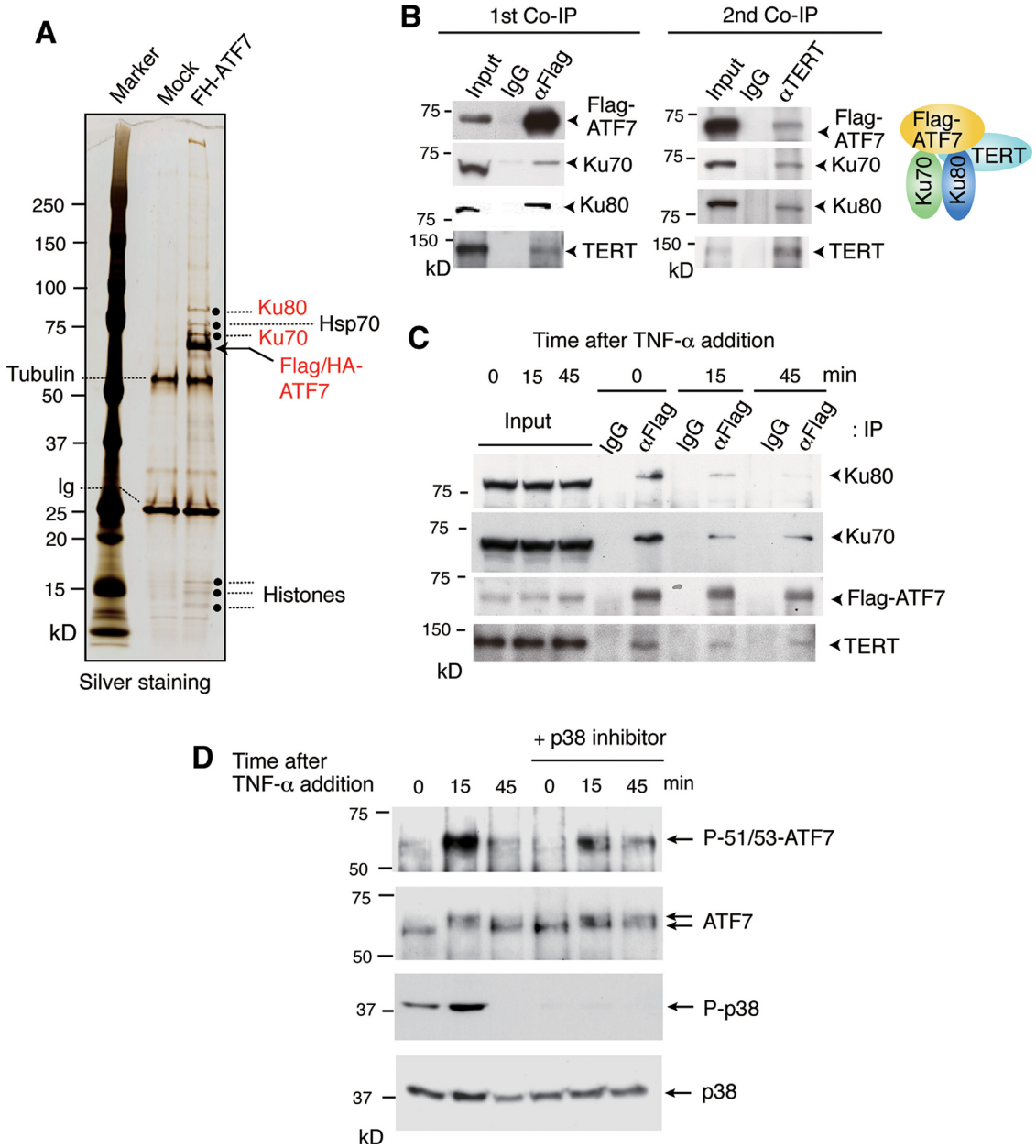


**Figure 4.** ATF7 interacts with Ku70/80 and TERT. (**A**) The ATF7 complex was immunopurified from HeLa cells expressing Flag/HA-tagged ATF7, resolved by SDS-PAGE, and visualized by silver staining. The polypeptides identified by mass-spectrometric analysis are indicated. (**B**) Two-step co-immunoprecipitation of the complex containing ATF7, Ku70/80 and TERT. Lysates from HeLa cells expressing Flag-HA–tagged ATF7 were first precipitated with anti-Flag antibody and eluted with Flag peptide; eluates were analyzed by western blotting to detect the proteins indicated on the right (first Co-IP). The anti-TERT monoclonal antibody (mAb) 2E4-2 was used to detect TERT. The eluates were then immunoprecipitated with anti-TERT mAb10E9-2 or control IgG, followed by western blotting (second Co-IP). Note that in the input lanes, endogenous TERT was immunoprecipitated with anti-hTERT mAb 10E9-2 and detected with mAb 2E4-2. (**C**) TNF-α disrupts the ATF7–Ku70/80–TERT complex. HeLa cells expressing Flag-HA–tagged ATF7 were treated with TNF-α for the indicated times, and then cell lysates were immunoprecipitated with anti-Flag, followed by western blotting to detect the proteins indicated on the right. To detect TERT, anti-TERT mAb 2E4-2 was used for western blotting. (**D**) TNF-α induces p38-dependent ATF7 phosphorylation. Nuclear extracts were prepared from HeLa S3 cells treated with TNF-α for the indicated times, and then subjected to western blotting with antibodies specific for the indicated proteins. In some cases, SB203580 (20 μM), an inhibitor of p38α and p38β, was added 2 h before addition of TNF-α. Based on the homology of the amino acid sequence around the phosphorylation sites between p38α, β, γ and δ, anti–phospho-p38 antibodies recognize P-p38α andβ, but may not recognize p38γ and δ. Therefore, the incomplete inhibition of TNF-α–induced phosphorylation of ATF7 may be due to the residual activities of p38γ and δ, which are not inhibited by SB203580.

results of binding assays using GST-ATF7 and 293T cell lysates with exogenously expressed EGFP-Ku70 fusion protein containing a series of C-truncated Ku70 (52) indicated that the C-terminal 390 amino acid region of Ku70 is important for interaction with ATF7 (Supplementary Figure S9C and D). This C-terminal region of Ku70 contains the SAP (after SAF-A/B, Acinus and PIAS) domain, which is thought to be involved in protein-protein interactions (53) in addition to DNA binding (54), and the Ku core domain, which is responsible for heterodimerization with Ku80 and binding to free DNA ends (55). This suggests that ATF7 binds to the SAP domain of the Ku heterodimer.

When Flag-ATF7 was immunoprecipitated by Flag antibody, Ku70/80 and TERT were co-precipitated (Figure 4C). When HeLa cells were exposed to TNF-α for 15 or 45 min, amount of co-precipitated Ku70/80 and TERT was decreased, indicating that TNF-α disrupted this ternary complex. It was also observed that ATF7 is phosphorylated by TNF-α treatment for 15 min, which was significantly reduced by the p38 inhibitor SB203580 (Figure 4D). It was reported that Thr-51 in ATF7 is phosphorylated by p38, whereas phosphorylation of Thr-53 by an unknown kinase is a prerequisite for p38 recruitment (56). ATF7 was transiently phosphorylated at 15 min after TNF-α addition, and phosphorylated ATF7 (pATF7) was not detected at 45 min after TNF-α addition (Figure 4D). Nevertheless, the ternary complex of ATF7, Ku70/80, and TERT was not detected at 45 min after TNF-α addition (Figure 4C), suggesting that this ternary complex is not re-formed immediately once it is disrupted.

### Localization of ATF7 and TERT to telomere via binding to the Ku complex

Since human Ku is associated with TERT (14) and telomeres (15), we examined whether ATF7 and TERT localize on telomere via binding to the Ku complex in HeLa cells using chromatin immunoprecipitation (ChIP) followed by slot-blot hybridization. Results using anti-ATF7 mAb 2F10 and anti-hTERT mAb 10E9-2, which was confirmed to immunoprecipitate endogenous hTERT (Supplementary Figure S7), demonstrated that ATF7 and TERT are localized on telomeres (Figure 5B). Knockdown of Ku70 using siRNA decreased the level of ATF7 and TERT on telomere (Figure 5A and B).

To further test this, MEFs from *Ku70*$^{-/-}$ mice were used. Since disagreeing results have been published regarding telomere shortening in *Ku70* or *Ku80* knockout mice (17,18), we made our own measurements by Q-PCR and Q-FISH. Results using both methods indicated that telomeres in *Ku70*-deficient MEFs were shorter than those in WT MEFs (Figure 5C and D and Supplementary Figure S10). To determine whether ATF7 localizes to telomeres via binding to Ku, we examined the amount of ATF7 on telomeres in *Ku70*$^{+/-}$ and *Ku70*$^{-/-}$ mouse lung epithelial (MLE) cell line derived from *Ku70* knockout mice (32) (Figure 5E). ChIP-seq/hybridization analysis revealed that less ATF7 was present on telomeres in *Ku70*-deficient cells than in *Ku70*$^{+/-}$ cells (Figure 5F), supporting a model in which ATF7 localizes to telomeres via binding to Ku (Figure 5G, left). Since Ku forms a complex with TRF1 (57) and TRF2 (58) at telomeres, Ku could be recruited to telomeres by interacting with TRF1 and TRF2, which directly binds to telomeres. In *Ku70*-deficient cells, about half amount of ATF7 was still retained on telomeres, suggesting the presence of another mechanism(s) underlying ATF7 is localized on telomeres. Since ATF7 interacts with histone tri-methyltransferase Suv39h1 and affects the level of H3K9me3 on telomeres (see below, Figure 8 and Supplementary Figure S12), ATF7 might be localized via uncharacterized factor(s) with Suv39h1 and histones (Figure 5G, right). This may be the reason why 60% of ATF7 is retained at telomeres in *Ku70*-deficient cells. We could not examine the amount of TERT on telomeres in those cells because no anti-mouse TERT antibody suitable for immunoprecipitation is currently available.

### TNF-α releases ATF7 and TERT from telomere through ATF7 phosphorylation

We next examined the effect of TNF-α on the levels of ATF7, TERT, and Ku70/Ku80 on telomeres by ChIP/slot-blot hybridization in HeLa cells, using specific antibodies against those proteins. TNF-α treatment induced a release of ATF7 and TERT, but not the Ku complex, from telomeres (Figure 6). In these experiments, we used the *Alu* repeat probe as a negative control and found that the ATF7, hTERT, and Ku70/80 signals on *Alu* repeats are much weaker than those on telomeres, indicating that those proteins on telomeres were specifically immunoprecipitated. At 45 min after TNF-α addition, a release of both ATF7 and TERT was observed, but only ATF7, but not TERT, was released at 15 min after TNF-α addition (Figure 6A and B). This suggests the presence of another mechanism of TERT recruitment to telomeres. It was reported that TERT is recruited to telomeres mainly through TPP1 (59–62). Therefore, since a role of ATF7 to recruit TERT to telomeres is relatively minor, TERT was not released from telomeres at 15 min after TNF-α addition even though some amount of ATF7 was released (see Discussion).

To further test whether ATF7 is really localized on telomeres, we performed the co-immunoprecipitation experiments of ATF7 and TRF2. Since the Ku complex was reported to bind to TRF1 (57) and TRF2 (58) on telomeres, ATF7 may indirectly interact with TRF2 via the Ku complex. Whole cell lysates were prepared from HeLa S3 cells expressing Flag-ATF7, and used for co-immunoprecipitation assays. Anti-Flag antibody, but not control IgG, co-immunoprecipitated TRF2 (Supplementary Figure S11). TNF-α treatment for 45 min reduced the amount of co-immunoprecipitated TRF2 by anti-Flag antibody. These results support the notion that ATF7 is localized on telomeres and is released by TNF-α treatment.

To investigate the potential effects of ATF7 phosphorylation on the level of TERT on telomeres, as well as the TNF-α–induced release of TERT from telomeres, we co-expressed HA-tagged TERT with ATF7 WT or T51/53A mutant, in which two phosphorylation sites were mutated to Ala, and then subjected the expressing cells to ChIP/slot-blot hybridization. Exogenous expression of ATF7 T51/53A blocked the TNF-α–induced release of TERT from telomere, although it decreased the level of

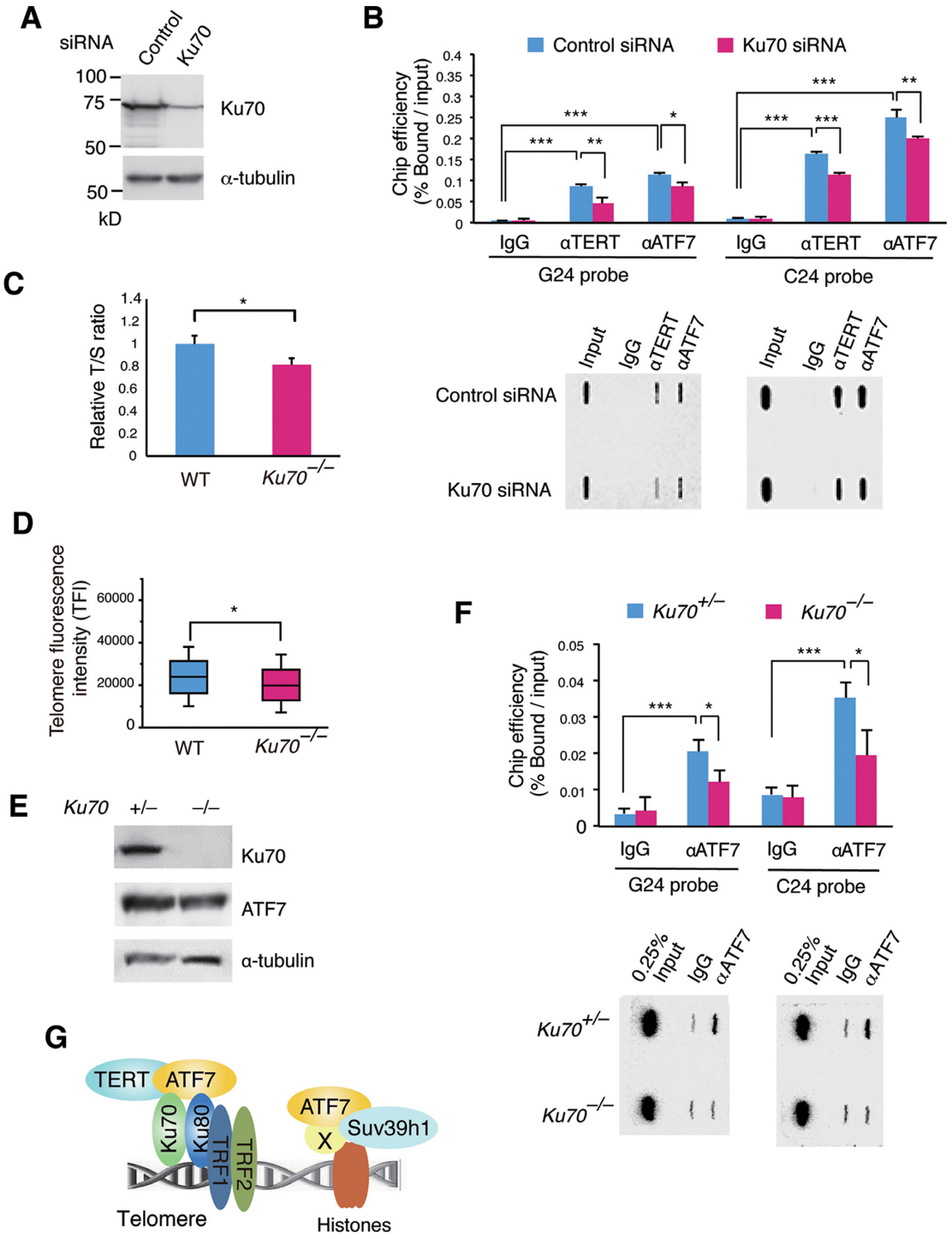


**Figure 5.** Localization of ATF7 and TERT to telomere via binding to the Ku complex. (**A**) Knockdown of Ku70 in HeLa cells. HeLa cells were transfected twice with Ku70 or control siRNA, and after 48 h cell lysates were subjected to western blotting. (**B**) Localization of ATF7 and TERT on telomere. Chromatin immunoprecipitation was performed using anti-TERT mAb 10E9-2 or anti-ATF7 antibodies, 72 h after transfection of Ku70 or control siRNA into HeLa cells. Recovered DNAs were subjected to slot-blot hybridization with a $^{32}$P-labeled telomere probe. Average signals are shown ± SD ($n = 3$), and typical data from slot-blot hybridization are shown below. $*P < 0.05$; $**P < 0.01$; $***P < 0.001$. (**C**, **D**) Telomere shortening in *Ku70*$^{-/-}$ MEFs. WT and *Ku70*$^{-/-}$ MEFs were used to measure telomere length using Q-PCR (C) or Q-FISH (D), and shown as described in Figure 1A, C. $*P < 0.05$. See Supplementary Figure S10A and B for control data of Q-PCR, and Supplementary Figure S10C and D for raw data of Q-FISH. (**E**) Loss of Ku70 in the *Ku70*$^{-/-}$ lung epithelial (MLE) cell line. *Ku70*$^{+/-}$ and *Ku70*$^{-/-}$ MLE cells were subjected to western blotting to detect the indicated proteins. (**F**) Loss of Ku70 decreases the level of ATF7 on telomere. *Ku70*$^{+/-}$ and *Ku70*$^{-/-}$ MLE cells were subjected to chromatin immunoprecipitation with anti-ATF7 antibody. Recovered DNA was subjected to slot-blot hybridization with a $^{32}$P-labeled telomere probe. Average signals are shown ± SD ($n = 3$), and typical data from slot-blot hybridization are shown in the lower panel. $*P < 0.05$; $***P < 0.001$. (**G**) Schematic showing the ATF7 complex on telomere. ATF7 localizes to telomeres via binding to Ku (left). Ku could be recruited to telomeres by interacting with TRF1 and TRF2 (57,58). Since ATF7 interacts with histone tri-methyltransferase Suv39h1, ATF7 might be also localized via uncharacterized factor(s) with Suv39h1 and histones (right).

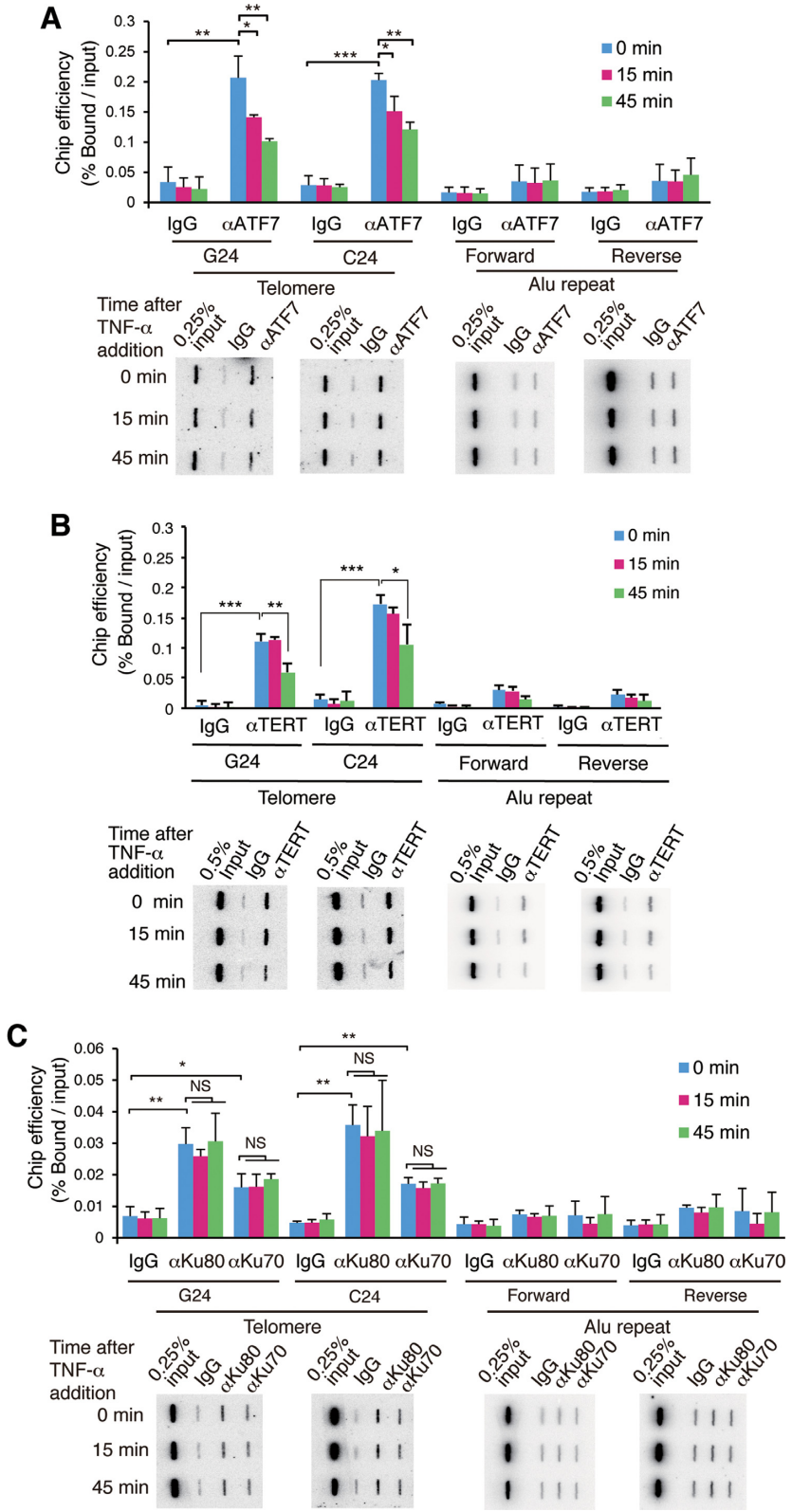


**Figure 6.** TNF-α releases ATF7 and TERT, but not Ku70/80 from telomere. (**A–C**) Effect of TNF-α treatment on ATF7, TERT, and Ku70/80 at telomere. HeLa cells treated with TNF-α (100 ng/ml) for the indicated time were used for ChIP/slot-blot hybridization with anti-ATF7 (A), anti-TERT mAb 10E9-2 (B), or anti-Ku70 and anti-Ku80 (C), as described in Figure 5B. A $^{32}$P-labeled *Alu* probe was used as a control. Average signals are shown ± SD ($n = 3$), and typical slot-blot hybridization data are shown below. *$P < 0.05$; **$P < 0.01$; ***$P < 0.001$; NS, not significant.

TERT on telomeres (Figure 7). Consistent with these results, exogenous expression of the ATF7 mutant T51/53A blocked the TNF-α–induced disruption of the complex containing ATF7, Ku complex, and TERT (Supplementary Figure S12A). In the absence of TNF-α treatment, the amount of ATF7 mutant T51/53A in the complex with Ku (Supplementary Figure S12A) was smaller than that of WT ATF7. This may suggest that the T51/53A mutation may slightly reduce the interaction with the Ku complex, which might also explain why expression of ATF7 mutant T51/53A decreased the level of TERT on telomeres. The slightly weaker interaction of T51/53A mutant with Ku70 compared to WT ATF7 was further supported by the GST pull-down assay (Supplementary Figure S12B). Thus, ATF7 is phosphorylated in response to TNF-α, resulting in release of ATF7 and TERT from telomeres and ultimately leading to telomere shortening.

### TNF-α reduces the H3K9me3 level on telomere via ATF7 phosphorylation

MEFs lacking two histone H3K9 tri-methyltransferases, Suv39h1 and Suv39h2, have longer telomeres than WT cells (63), suggesting that reduction of the H3K9me3 level induces telomere lengthening. Because the *Drosophila* and yeast orthologs of ATF7 (dATF2 and Atf1) regulate the H3K9me3 level on heterochromatin (27,28), we investigated the possibility that ATF7 mediates telomere shortening by affecting H3K9me3 levels on the telomeres. Quantitative ChIP assays using anti-histone H3 and anti-H3K9me3 antibodies revealed that the H3K9me3 level on telomeres and centromeric heterochromatin was lower in *Atf7*$^{-/-}$ MEFs than in WT MEFs (Figure 8A and Supplementary Figure S13A). TNF-α treatment decreased the H3K9me3 level on telomeres and centromeric heterochromatin in WT MEFs, but not in *Atf7*$^{-/-}$cells (Figure 8A and Supplementary Figure S13A). TNF-α also reduced the H3K9me3 level on telomeres in HeLa cells (Figure 8B). Consistent with this, the intensity of H3K9me3 immunostaining was lower in *Atf7*$^{-/-}$MEFs than in WT cells (Supplementary Figure S13B). Furthermore, co-immunoprecipitation experiments revealed that ATF7 interacts with Suv39h1; this interaction was not disrupted following TNF-α treatment (Figure 8C and Supplementary Figure S13C). The results of ChIP/slot-blot hybridization demonstrated that Suv39h1 is localized on telomeres in WT MEFs, but not in *Atf7*$^{-/-}$MEFs (Figure 8D), suggesting that Suv39h1 binds to telomeres via ATF7. Furthermore, in WT MEFs, Suv39h1 was released from telomeres by TNF-α (Figure 8D), suggesting that ATF7 and Suv39h1 are released together from telomeres in response to TNF-α treatment. The ChIP assays showed that ATF7 also binds to pericentromeric heterochromatin regions, and that both ATF7 and Suv39h1 are released from pericentromeric heterochromatin by TNF-α (Supplementary Figure S13D). In light of the observation that Suv39h1/2 mutations induce telomere lengthening (63), it is possible that the TNF-α−induced decrease in H3K9me3 on telomeres may cause telomere lengthening in a similar manner. Together, these findings suggest that TNF-α–induced telomere shortening is caused by release of ATF7/TERT from telomeres, rather than by altering the level of H3K9me3.

## DISCUSSION

### Mechanism of TNF-α-induced telomere shortening and its significance

In this study, we demonstrated that ATF7 and telomerase localize to telomeres by direct binding to the Ku complex under unstressed conditions, thus preventing telomere shortening (Figure 9A, left). It is well known that telomerase is mainly recruited to telomeres through and interaction between the TEN domain of telomerase and the TEL patch of TPP1 (Figure 9A, right) (59–62). Therefore, the role of ATF7-Ku pathway may be a relatively minor to recruit telomerase to telomeres, which is consistent with the mild telomere shortening caused by a loss of ATF7 and TNF-α treatment. However, this pathway may have the important physiological role. In response to TNF-α treatment, ATF7 is phosphorylated and released from telomeres together with telomerase. Thus, ATF7 knockout or knockdown mimics the stressed state. Results of co-immunoprecipitation experiments suggested that the Ku-ATF7-telomerase ternary complex does not re-form immediately after it is disrupted. This suggests that daily TNF-α treatment of pregnant mice or cultured cells generates telomeres with decreased telomerase for prolonged periods, which leads to telomere shortening. Shorter telomeres in *Atf7*$^{-/-}$cells than in WT cells may support this model.

The TNF-α treatment induced a decrease in H3K9me3 on telomeres, which is caused by a release of the ATF7-Suv39h1 complex. This may cause telomere lengthening, because Suv39h1/2 mutations induce telomere lengthening (63) (Figure 9B, right). Thus, the TNF-α treatment may induce telomere shortening and lengthening by a release of ATF7-telomerase and ATF7-Suv39h1, respectively (Figure 9B). The observation that the TNF-α treatment caused telomere shortening, not telomere lengthening, may indicate that the degree of telomere shortening is bigger than that of telomere lengthening.

Physiological role of mild telomere shortening in *Atf7*$^{-/-}$ mice is unknown at present. Since telomere shortening is associated with changes in cellular metabolism (6), such mild telomere shortening may also affect metabolism and associated phenotype(s). *Atf7*$^{-/-}$ mice exhibited slightly lower body weight compared with that of WT mice, and resisted diet-induced obesity (64), which may suggest the possibility that the involvement of telomere shortening in adipocyte differentiation and/or maintenance and metabolism. Further analysis is required for understanding the physiological role of telomere shortening in *Atf7*$^{-/-}$ mice.

ATF7 is required for heterochromatin formation by recruiting histone H3K9 trimethyltransferase Suv39h1 and for the formation of heterochromatin-like structure in euchromatin region by recruiting histone H3K9 dimethyltransferase G9a (26). ATF7 also protects the telomere and prevents its shortening by recruiting telomerase. Thus, ATF7 contributes to make the silent and tight chromatin structure at both heterochromatin and telomeres. On the other hand, ATF7 has seemingly opposite roles in tight

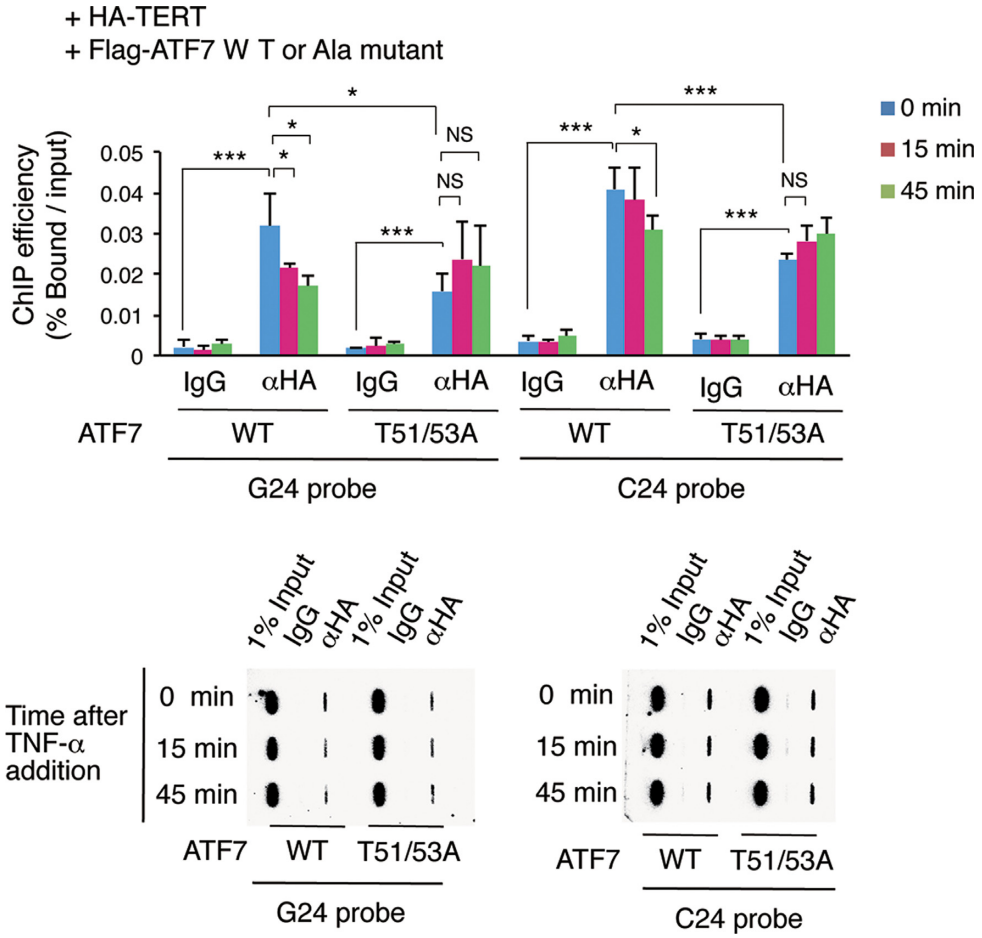


**Figure 7.** T51/53A, a phosphorylation-site mutant of ATF7, blocks TNF-α–induced release of TERT from telomeres. HeLa cells were transfected with plasmids for expression of HA-hTERT and Flag-tagged ATF7 WT or T51/53A mutant. Forty-eight hours after transfection, cells were treated with TNF-α for the indicated times, and then subjected to ChIP/slot-blot hybridization with anti-HA antibody. Average signals ± SD ($n = 4$) are shown below, and typical slot-blot hybridization data are shown on the right. *$P < 0.05$; **$P < 0.01$; ***$P < 0.001$; NS, not significant.

chromatin structure formation and mediates the stress-induced disruption of heterochromatin and the TNF-α-induced telomere shortening. It is interesting why the organisms have such system in which ATF7 has opposite roles. One possibility is that this system may be selected during evolution because of its beneficial role in the generation of diversity, followed by selection. The ATF7-mediated heterochromatin disruption and telomere shortening in response to various stresses may accelerate the rate of mutation including chromosome structure changes, which might enhance the diversity of the genome. In fact, a disruption of heterochromatin causes transposon mobilization (65), while telomere shortening increases mutation rate and chromosome instability (66). In additon, the ATF7-mediated change of chromatin structure in response to various types of stress could be beneficial to adapt to environmental conditions and have an advantage to survive. The pathogen infection-induced and ATF7-mediated disruption of heterochromatin-like structure in macrophages is retained for long period and increases the resistance to pathogen attack (26). The stress-induced telomere shortening may be also maintained for long period. It was shown that telomere shortening decreases mitochondrial biogenesis and gluconeogenesis (6). The decrease in metabolism might play a positive role to survive after receiving stress.

Anxiety has been associated with accelerated aging (67). Epidemiological studies have also suggested that some social stressors shorten telomere length (7,8). However, a rigorous connection has not been established between these two phenomena. In part, this is because the relationship between social stress and telomere length has not been widely accepted, due largely to the fact that the mechanism is unknown. The prtesent study clarifies the mechanism by which certain types of stress might shorten telomere length, giving credence to the idea that various types of stress might shorten telomere length. Thus, clarification of the mechanism of stress-induced telomere shortening contributes to understanding of the relationship between stress and telomere shortening.

### Reliability of telomere shortening and association among ATF7, Ku70/80 and TERT

The degree of telomere shortening by a loss of ATF7 or by TNF-α treatment was mild, raised the possibility that this might be within the measurement error. To test whether

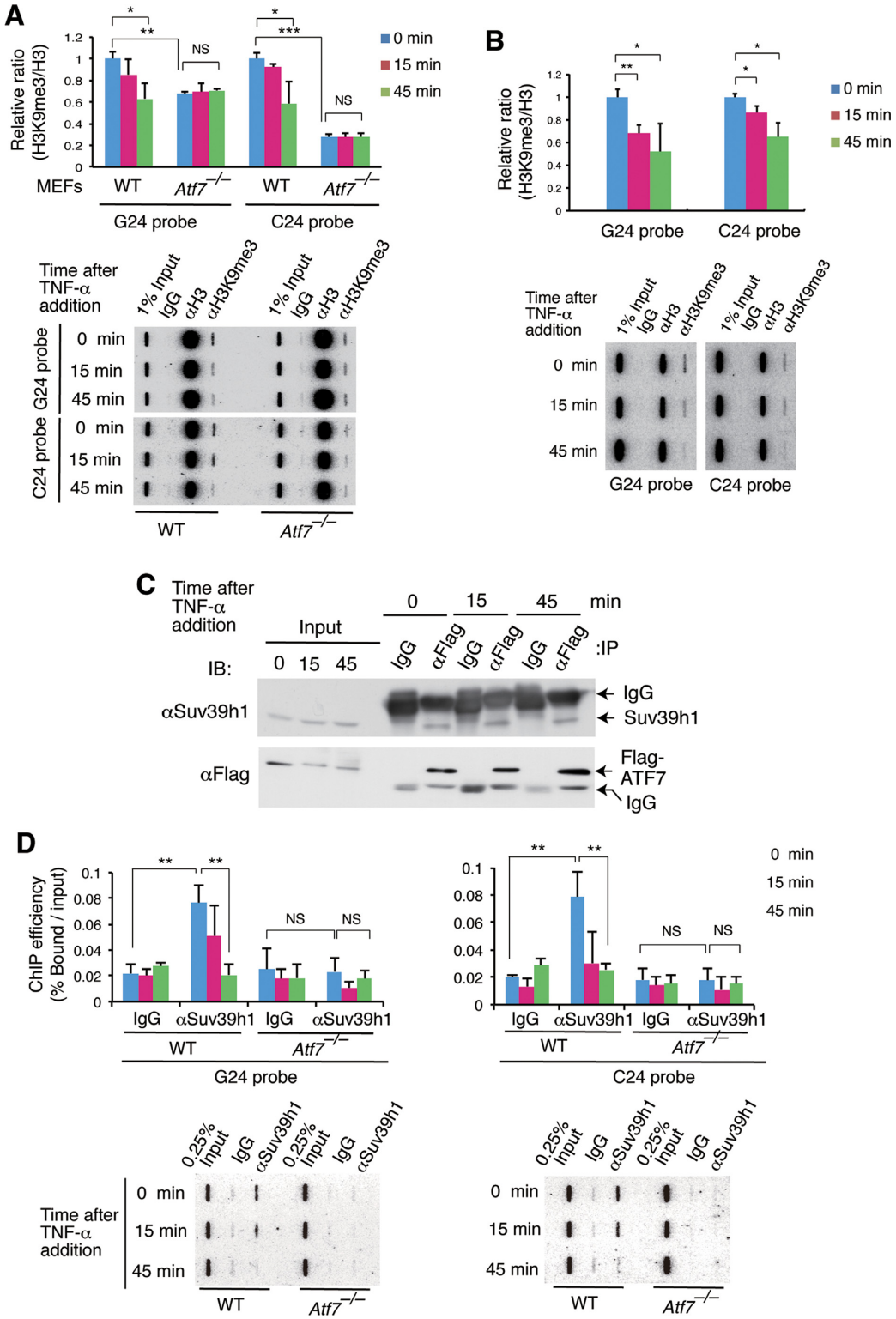


**Figure 8.** ATF7 mediates telomere shortening not by regulating H3K9me3 level. (**A**, **B**) ATF7 mediates a TNF-α–induced decrease in histone H3K9me3 levels on telomeres. WT or *Atf7*$^{-/-}$ MEFs (A), or HeLa cells (B), were treated with TNF-α for the indicated times, and ChIP/slot-blot hybridization was performed using anti-histone H3 and anti-H3K9me3 antibodies with the telomere probe. Average H3K9me3/H3 ratios are shown ± SD ($n = 3$), and typical slot-blot hybridization data are shown below. *$P < 0.05$; NS, not significant. (**C**) Interaction between ATF7 and Suv39h1 is not abrogated by TNF-α treatment. HeLa cells expressing Flag-ATF7 were treated with TNF-α (100 ng/ml) for the indicated times; whole-cell lysates were prepared and immunoprecipitated with anti-ATF7; and the immunoprecipitates were immunoblotted with anti-Suv39h1 antibody. (**D**) Release of Suv39h1 from telomere following TNF-α treatment. WT or *Atf7*$^{-/-}$ MEFs were treated with TNF-α (100 ng/ml) for the indicated times, and then subjected to ChIP/slot-blot hybridization using anti-Suv39h1 antibodies and telomeric probes. Average signals ± SD ($n = 3$) are shown below. *$P < 0.05$; **$P < 0.01$; NS, not significant.

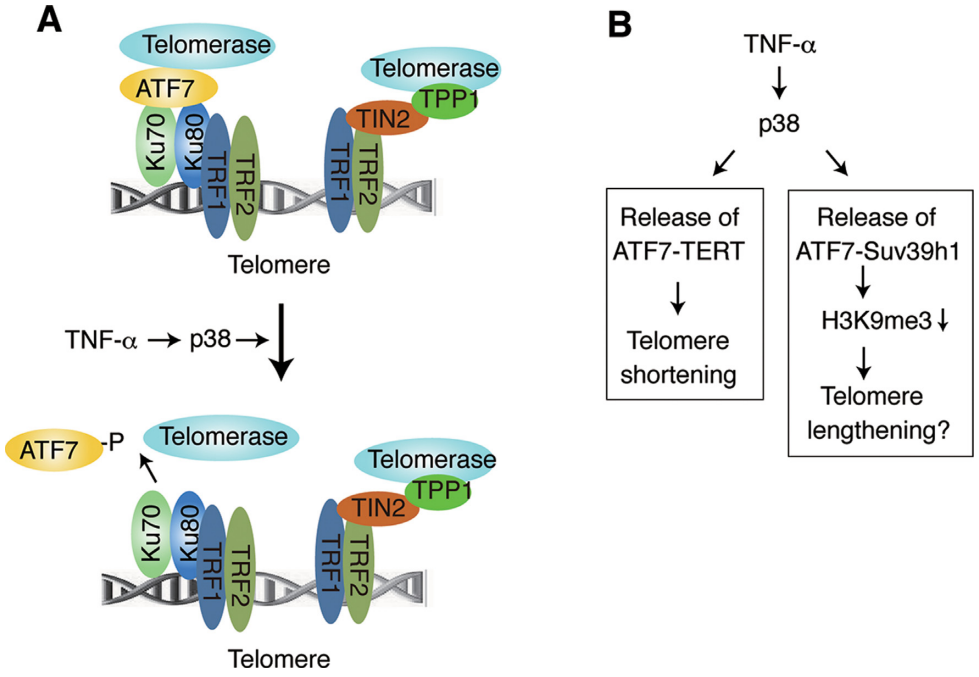


**Figure 9.** Model of TNF-α–induced telomere shortening. (**A**) Schematic showing the release of ATF7 and telomerase from telomeres following TNF-α treatment. (Left) ATF7 and telomerase localize to telomeres by binding to the Ku complex under unstressed conditions. In response to TNF-α treatment, ATF7 is phosphorylated and released from telomeres together with telomerase. (Right) In addition, telomerase is mainly recruited to telomeres through TPP1 (59–62). Therefore, the role of ATF7-Ku pathway may be a relatively minor to recruit telomerase to telomeres. (**B**) Schematic view of the effect of TNF-α on telomere length and H3K9me3. (Left) The TNF-α treatment induces telomere shortening by a release of ATF7-telomerase. (Right) The TNF-α treatment induces a release of the ATF7-Suv39h1 complex, leading to a decrease in H3K9me3 on telomeres. This may cause telomere lengthening, because Suv39h1/2 mutations induce telomere lengthening (63). These two mechanisms may work competitively.

this measurement of telomere shortening was correct, we used three independent MEF preparations from independent pregnant mice to eliminate the effects of mouse-to-mouse variation. We also used MEFs from the fourth generation of *Tert*$^{-/-}$ mice as a control to show that TNF-α–induced telomere shortening is telomerase-dependent. Furthermore, we used not only MEFs but also HeLa cells, and measured telomere length using three different methods, Q-FISH, Q-PCR, and TRF assays.

Ku70/80 are the abundant proteins, raised the possibility that Ku70/80 were non-specifically associated with ATF7 during purification of the ATF7 complex. However, Ku proteins were not detected in the Ski corepressor complex, which was purified using the same 300 mM salt condition (37), suggesting that the Ku complex specifically associates with ATF7. To further demonstrate that Ku is not a contaminating protein, we used HeLa cells expressing Flag-Ski transcriptional corepressor as the control for co-immunoprecipitation experiments. Under the same co-immunoprecipitation conditions, Ku proteins co-precipitated with ATF7, but not with Ski, suggesting that Ku specifically interacts with ATF7. It was shown that Ku proteins are localized on telomeres in human cells using ChIP assay (15,17). Although such data has not been obtained using mouse cells, we have now shown that Ku proteins are localized on telomeres in mouse lung epithelial cells using ChIP. These results support the notion that Ku proteins are localized on telomeres also in mice. Furthermore, to determine whether ATF7 localizes to telomeres via binding to Ku, we have shown that less ATF7 was present on telomeres in *Ku70*-deficient mouse lung epithelial cells than in WT cells, supporting a model in which ATF7 localizes to telomeres via binding to Ku. Ku localizes to the nucleus and has many functions including DNA repair. Since Ku forms a complex with TRF1 and TRF2 at telomeres (57,58), small amount of Ku could be specifically recruited to telomeres by interacting with TRF1 and TRF2, which directly binds to telomeres. Such mechanism may help the interaction between some fraction of abundant Ku proteins with small amount of telomerase.

TERT is not abundant, and western and ChIP of TERT have not been trustable as shown by many groups. We (Masutomi and colleagues) recently generated a series of mAbs against hTERT (39), and have confirmed that endogenous hTERT can be detected by immunoprecipitation with anti-hTERT mAb 10E9-2 followed by immunoblotting with anti-hTERT mAb 2E4-2. Using these antibodies, we confirmed the association among hTERT, ATF7, and Ku70/80, and performed ChIP to show that hTERT is localized on telomeres. We also found that the ATF7, hTERT, and Ku70/80 signals on *Alu* repeats are much weaker than those on telomeres, supporting the notion that TERT on telomeres were specifically immunoprecipitated.

### Difference between *Atf7*- and telomerase-deficient mice

The length of telomeres in telomerase-deficient mice decreases with increasing generations, and skin lesions in epidermal hyperplasia and hyperkeratosis as well as the failure

of neural tube closure are evident in the fourth to sixth generation (G4–G6) of telomerase-deficient mice (41,68). However, the degree of telomere shortening in *Atf7*$^{-/-}$ mice did not increase with increasing generations, and no abnormality such as skin lesions or failure of neural tube closure was observed even in the 12th generation (G12) of *Atf7*$^{-/-}$ mice. This may be because normal levels of telomerase expression are maintained and telomerase is recruited to telomeres via TPP1 in *Atf7*$^{-/-}$ mice (Figure 9A, right), despite a reduced amount of telomerase on telomeres in *Atf7*$^{-/-}$ mice. Telomere length is reset during mouse early embryogenesis through both telomerase-dependent and telomerase-independent mechanisms via recombination (ALT: alternative lengthening of telomeres) (69,70). This process may reset telomere length that is mildly shortened by stress or loss of ATF7, and resetting of telomere length might be abrogated or only partial in telomerase-deficient mice. Thus, we speculate that continuous crossing of *Atf7*$^{-/-}$ mice do not exacerbate telomere shortening because these animals have normal level of telomerase expression which is recruited to telomeres via TPP1.

### Mixing of information obtained using different systems

Originally, the psychological stress-induced telomere shortening was suggested by the epidemiological studies of human being. In the present study, we first used mice to examine the TNF-α-induced telomere shortening, and then used human cells to analyze the mechanism. This was because the antibody to detect endogenous mouse TERT is not available at present, and our monoclonal antibodies can detect only hTERT, but not mTERT. It is potentially dangerous to mix information obtained using different systems. However, to elucidate the mechanism of a complex phenomenon, such as psychological stress-induced telomere shortening, a model system such as mouse is very useful. For this reason, here we used TNF-α injection into mice, because many papers reported that various psychological stresses increase the TNF-α level in peripheral tissues (42). Thus, in this study, we combined the role of psychological stress (mimicked by TNF-α), Ku complex, and ATF7 in the mouse system. The role of Ku complex in recruiting TERT to telomere was clearly demonstrated in yeast, whereas it remains unclear whether the complex plays a similar role in mice and human. However, it was shown that Human Ku is associated with human TERT (hTERT) (14). Furthermore, localization of the Ku complex on telomeres in human cells was shown by ChIP assay (15,17), possibly via TRF1 and TRF2 (57,58). We have also demonstrated that Ku is localized on telomeres in mouse cells by ChIP assay in this study. Disagreeing results have been published regarding telomere shortening in *Ku70* or *Ku80* knockout mice (17,18). To test whether a loss of Ku70 causes telomere shortening, we made our own measurements by Q-PCR and Q-FISH, and found that telomeres in *Ku70*-deficient MEFs were shorter than those in WT MEFs, providing independent confirmation that Ku is involved in the regulation of telomere length in mice. Thus, based on those evidences, we speculated that the results from mouse and human cells are interchangeable.

The members of the ATF2 subfamily of transcription factors, including ATF7, are phosphorylated in response to a variety of stresses (23). Therefore, it is likely that telomere shortening is induced by various stresses through similar mechanisms. Further studies will be required to understand whether stress-induced telomere shortening is linked to specific diseases.

## SUPPLEMENTARY DATA

Supplementary Data are available at NAR Online.

## ACKNOWLEDGEMENTS

We are grateful to the staff of the Research Resources Center of the RIKEN Brain Science Institute for assistance with mass-spectrometric analysis; to Y. Nakatani for pOZ-FH-N vector; to F. Alt for *Ku70* knockout mice; and to H. Seimiya for the hTERT expression vector.

## FUNDING

Japan Agency for Medical Research and Development (AMED) [16gm0510015h0004]; Ministry of Education, Culture, Sports, Science and Technology (MEXT) [16H01413]. Funding for open access charge: Japan Agency for Medical Research and Development (AMED).
*Conflict of interest statement.* None declared.

## REFRERENCES

1. Blackburn,E.H. (2001) Switching and signaling at the telomere. *Cell*, **106**, 661–673.
2. Palm,W. and de Lange,T. (2008) How shelterin protects mammalian telomeres. *Annu. Rev. Genet.*, **42**, 301–334.
3. Harley,C.B., Futcher,A.B. and Greider,C.W. (1990) Telomeres shorten during ageing of human fibroblasts. *Nature*, **345**, 458–460.
4. Smogorzewska,A. and de Lange,T. (2004) Regulation of telomerase by telomeric proteins. *Annu. Rev. Biochem.*, **73**, 177–208.
5. Blasco,M.A. (2005) Telomeres and human disease: ageing, cancer and beyond. *Nat. Rev. Genet.*, **6**, 611–622.
6. Sahin,E., Colla,S., Liesa,M., Moslehi,J., Müller,F.L., Guo,M., Cooper,M., Kotton,D., Fabian,A.J., Walkey,C. *et al.* (2011) Telomere dysfunction induces metabolic and mitochondrial compromise. *Nature*, **470**, 359–365.
7. Epel,E.S., Blackburn,E.H., Lin,J., Dhabhar,F.S., Adler,N.E., Morrow,J.D. and Cawthon,R.M. (2004) Accelerated telomere shortening in response to life stress. *Proc. Natl. Acad. Sci. U.S.A.*, **101**, 17312–17315.
8. Entringer,S., Epel,E.S., Kumsta,R., Lin,J., Hellhammer,D.H., Blackburn,E.H., Wüst,S. and Wadhwa,P.D. (2011) Stress exposure in intrauterine life is associated with shorter telomere length in young adulthood. *Proc. Natl. Acad. Sci. U.S.A.*, **108**, E513–E518.
9. von Zglinicki,T. (2002) Oxidative stress shortens telomeres. *Trends Biochem. Sci.*, **27**, 339–344.
10. Stellwagen,A.E., Haimberger,Z.W., Veatch,J.R. and Gottschling,D.E. (2003) Ku interacts with telomerase RNA to promote telomere addition at native and broken chromosome ends. *Genes Dev.*, **17**, 2384–2395.
11. Fisher,T.S., Taggart,A.K. and Zakian,V.A. (2014) Cell cycle-dependent regulation of yeast telomerase by Ku. *Nat. Struct. Mo.l Biol.*, **11**, 1198–1205.
12. Lopez,C.R., Ribes-Zamora,A., Indiviglio,S.M., Williams,C.L., Haricharan,S. and Bertuch,A.A. (2011) Ku must load directly onto the chromosome end in order to mediate its telomeric functions. *PLoS Genet.*, **7**, e1002233.
13. Pfingsten,J.S., Goodrich,K.J., Taabazuing,C., Ouenzar,F., Chartrand,P. and Cech,T.R. (2012) Mutually exclusive binding of telomerase RNA and DNA by Ku alters telomerase recruitment model. *Cell*, **148**, 922–932.

14. Chai,W., Ford,L.P., Lenertz,L., Wright,W.E. and Shay,J.W. (2002) Human Ku70/80 associates physically with telomerase through interaction with hTERT. *J. Biol. Chem.*, **277**, 47242–47247.
15. Hsu,H.L., Gilley,D., Blackburn,E.H. and Chen,D.J. (1999) Ku is associated with the telomere in mammals. *Proc. Natl. Acad. Sci. U.S.A.*, **96**, 12454–12458.
16. Wang,Y., Ghosh,G. and Hendrickson,E.A. (2009) Ku86 represses lethal telomere deletion events in human somatic cells. *Proc. Natl. Acad. Sci. U.S.A.*, **106**, 12430–12435.
17. d'Adda di Fagagna,F., Hande,M.P., Tong,W.M., Roth,D., Lansdorp,P.M., Wang,Z.Q. and Jackson,S.P. (2001) Effects of DNA nonhomologous end-joining factors on telomere length and chromosomal stability in mammalian cells. *Curr. Biol.*, **11**, 1192–1196.
18. Espejel,S., Franco,S., Rodríguez-Perales,S., Bouffler,S.D., Cigudosa,J.C. and Blasco,M.A. (2002) Mammalian Ku86 mediates chromosomal fusions and apoptosis caused by critically short telomeres. *EMBO J.*, **21**, 2207–2219.
19. Gaire,M., Chatton,B. and Kedinger,C. (1990) Isolation and characterization of two novel, closely related ATF cDNA clones from HeLa cells. *Nucleic Acids Res.*, **18**, 3467–3473.
20. Maekawa,T., Sakura,H., Kanei-Ishii,C., Sudo,T., Yoshimura,T., Fujisawa,J., Yoshida,M. and Ishii,S. (1989) Leucine zipper structure of the protein CRE-BP1 binding to the cyclic AMP response element in brain. *EMBO J.*, **8**, 2023–2028.
21. Hai,T.W., Liu,F., Coukos,W.J. and Green,M.R. (1989) Transcription factor ATF cDNA clones: an extensive family of leucine zipper proteins able to selectively form DNA-binding heterodimers. *Genes Dev.*, **3**, 2083–2090.
22. Gupta,S., Campbell,D., Dérijard,B. and Davis,R.J. (1995) Transcription factor ATF2 regulation by the JNK signal transduction pathway. *Science*, **267**, 389–393.
23. Seong,K.H., Maekawa,T. and Ishii,S. (2012) Inheritance and memory of stress-induced epigenome change: roles played by the ATF-2 family of transcription factors. *Genes Cells*, **17**, 249–263.
24. Maekawa,T., Kim,S., Nakai,D., Makino,C., Takagi,T., Ogura,H., Yamada,K., Chatton,B. and Ishii,S. (2010) Social isolation stress induces ATF-7 phosphorylation and impairs silencing of the 5-HT 5B receptor gene. *EMBO J.*, **29**, 196–208.
25. Wang,H., An,W., Cao,R., Xia,L., Erdjument-Bromage,H., Chatton,B., Tempst,P., Roeder,R.G. and Zhang,Y. (2003) mAM facilitates conversion by ESET of dimethyl to trimethyl lysine 9 of histone H3 to cause transcriptional repression. *Mol. Cell*, **12**, 475–487.
26. Yoshida,K., Maekawa,T., Zhu,Y., Renard-Guillet,C., Chatton,B., Inoue,K., Uchiyama,T., Ishibashi,K., Yamada,T., Ohno,N. *et al.* (2015) The transcription factor ATF7 mediates lipopolysaccharide-induced epigenetic changes in macrophages involved in innate immune memory. *Nat. Immunol.*, **16**, 1034–1043.
27. Seong,K.H., Li,D., Shimizu,H., Nakamura,R. and Ishii,S. (2011) Inheritance of stress-induced, ATF-2-dependent epigenetic change. *Cell*, **145**, 1049–1061.
28. Jia,S., Noma,K. and Grewal,S.I. (2004) RNAi-independent heterochromatin nucleation by the stress-activated ATF/CREB family proteins. *Science*, **304**, 1971–1976.
29. Liu,B., Maekawa,T., Chatton,B. and Ishii,S. (2006) In utero TNF-α treatment induces telomere shortening in young adult mice in an ATF7-dependent manner. *FEBS Open Biol.*, **6**, 56–63.
30. Yuan,X., Ishibashi,S., Hatakeyama,S., Saito,M., Nakayama,J., Nikaido,R., Haruyama,T., Watanabe,Y., Iwata,H., Iida,M. *et al.* (1999) Presence of telomeric G-strand tails in the telomerase catalytic subunit TERT knockout mice. *Genes Cells*, **4**, 563–572.
31. Gu,Y., Seidl,K.J., Rathbun,G.A., Zhu,C., Manis,J.P., van der Stoep,N., Davidson,L., Cheng,H.L., Sekiguchi,J.M., Frank,K. *et al.* (1997) Growth retardation and leaky SCID phenotype of *Ku70*-deficient mice. *Immunity*, **7**, 653–665.
32. Koike,M., Yutoku,Y. and Koike,A. (2011) Establishment of *ku*70-deficient lung epithelial cell lines and their hypersensitivity to low-dose x-irradiation. *J. Vet. Med. Sci.*, **73**, 549–554.
33. Takubo,K., Aida,J., Izumiyama,N., Ishikawa,N., Fujiwara,M., Poon,S.S., Kondo,H., Kammori,M., Matsuura,M., Sawabe,M. *et al.* (2010) Chromosomal instability and telomere lengths of each chromosomal arm measured by Q-FISH in human fibroblast strains prior to replicative senescence. Mech. *Ageing Dev.*, **131**, 614–624.
34. Poon,S.S. and Lansdorp,P.M. (2001) Quantitative fluorescence in situ hybridization (Q-FISH). *Curr. Protoc. Cell Biol.*, doi:10.1002/0471143030.cb1804s12.
35. Cawthon,R.M. (2002) Telomere measurement by quantitative PCR. *Nucleic Acids Res.*, **30**, e47.
36. Callicott,R.J. and Womack,J.E. (2006) Real-time PCR assay for measurement of mouse telomeres. *Comp. Med.*, **56**, 17–22.
37. Tabata,T., Kokura,K., Ten Dijke,P. and Ishii,S. (2009) Ski co-repressor complexes maintain the basal repressed state of the TGF-β target gene, SMAD7, via HDAC3 and PRMT5. *Genes Cells*, **14**, 17–28.
38. Dignam,J.D., Lebovitz,R.M. and Roeder,R.G. (1983) Accurate transcription initiation by RNA polymerase II in a soluble extract from isolated mammalian nuclei. *Nucleic Acids Res.*, **11**, 1475–1489.
39. Maida,Y., Yasukawa,M., Okamoto,N., Ohka,S., Kinoshita,K., Totoki,Y., Ito,T.K., Minamino,T., Nakamura,H., Yamaguchi,S. *et al.* (2014) Involvement of telomerase reverse transcriptase in heterochromatin maintenance. *Mol. Cell. Biol.*, **34**, 1576–1593.
40. Okamoto,N., Yasukawa,M., Nguyen,C., Kasim,V., Maida,Y., Possemato,R., Shibata,T., Ligon,K.L., Fukami,K., Hahn,W.C. *et al.* (2011) Maintenance of tumor initiating cells of defined genetic composition by nucleostemin. *Proc. Natl. Acad. Sci. U.S.A.*, **108**, 20388–20393.
41. Rudolph,K.L, Chang,S., Lee,H.W., Blasco,M., Gottlieb,G.J., Greider,C. and DePinho,R.A. (1999) Longevity, stress response, and cancer in aging telomerase-deficient mice. *Cell*, **96**, 701–712.
42. Maes,M., Song,C., Lin,A., De Jongh,R., Van Gastel,A., Kenis,G., Bosmans,E., De Meester,I., Benoy,I., Neels,H. *et al.* (1998) The effects of psychological stress on humans: increased production of pro-inflammatory cytokines and a Th1-like response in stress-induced anxiety. *Cytokine*, **10**, 313–318.
43. Sass,G., Shembade,N.D. and Tiegs,G. (2005) Tumour necrosis factor alpha (TNF)-TNF receptor 1-inducible cytoprotective proteins in the mouse liver: relevance of suppressors of cytokine signalling. *Biochem. J.*, **385**, 537–544.
44. Blasco,M.A., Lee,H.W., Hande,M.P., Samper,E., Lansdorp,P.M., DePinho,R.A. and Greider,C.W. (1997) Telomere shortening and tumor formation by mouse cells lacking telomerase RNA. *Cell* **91**, 25–34.
45. Lee,H.W., Blasco,M.A., Gottlieb,G.J., Horner,J.W. II, Greider,C.W. and DePinho,R.A. (1998) Essential role of mouse telomerase in highly proliferative organs. *Nature* **392**, 569–574.
46. Akiyama,M., Hideshima,T., Hayashi,T., Tai,Y.T., Mitsiades,C.S., Mitsiades,N., Chauhan,D., Richardson,P., Munshi,N.C. and Anderson,K.C. (2003) Nuclear factor-κB p65 mediates tumor necrosis factor α-induced nuclear translocation of telomerase reverse transcriptase protein. *Cancer Res.*, **63**, 18–21.
47. Seimiya,H., Sawada,H., Muramatsu,Y., Shimizu,M., Ohko,K., Yamane,K. and Tsuruo,T. (2000). Involvement of 14-3-3 proteins in nuclear localization of telomerase. *EMBO J.*, **19**, 2652–2661.
48. Liu,P., Lu,M., Tian,B., Li,K., Garofalo,R.P., Prusak,D., Wood,T.G. and Brasier,A.R. (2009) Expression of an IKKγ splice variant determines IRF3 and canonical NF-κB pathway utilization in ssRNA virus infection. *PLoS One* **4**, e8079.
49. Stiff,T., Walker,S.A., Cerosaletti,K., Goodarzi,A.A., Petermann,E., Concannon,P., O'Driscoll,M. and Jeggo,P.A. (2006) ATR-dependent phosphorylation and activation of ATM in response to UV treatment or replication fork stalling. *EMBO J.*, **25**, 5775–5782.
50. Beck,M., Schmidt,A., Malmstroem,J., Claassen,M., Ori,A., Szymborska,A., Herzog,F., Rinner,O., Ellenberg,J. and Aebersold,R. (2011) The quantitative proteome of a human cell line. *Mol. Syst. Biol.*, **7**, 549.
51. Sano,Y., Harada,J., Tashiro,S., Gotoh-Mandeville,R., Maekawa,T. and Ishii,S. (1999) ATF-2 is a common nuclear target of Smad and TAK1 pathways in transforming growth factor-β signaling. *J. Biol. Chem.*, **274**, 8949–8957.
52. Koike,M., Ikuta,T., Miyasaka,T. and Shiomi,T. (1999) The nuclear localization signal of the human Ku70 is a variant bipartite type recognized by the two components of nuclear pore-targeting complex. *Exp. Cell Res.*, **250**, 401–413.
53. Fekairi,S., Scaglione,S., Chahwan,C., Taylor,E.R., Tissier,A., Coulon,S., Dong,M.Q., Ruse,C., Yates,J.R. 3rd, Russell,P. *et al.* (2009) Human SLX4 is a Holliday junction resolvase subunit that

binds multiple DNA repair/recombination endonucleases. *Cell*, **138**, 78–89.
54. Aravind,L. and Koonin,E.V. (2000) SAP - a putative DNA-binding motif involved in chromosomal organization. *Trends Biochem. Sci.*, **25**, 112–114.
55. Walker,J.R., Corpina,R.A. and Goldberg,J. (2001) Structure of the Ku heterodimer bound to DNA and its implications for double-strand break repair. *Nature*, **412**, 607–614.
56. Camuzeaux,B., Diring,J., Hamard,P.J., Oulad-Abdelghani,M., Donzeau,M., Vigneron,M., Kedinger,C. and Chatton,B. (2008) p38β2-mediated phosphorylation and sumoylation of ATF7 are mutually exclusive. *J. Mol. Biol.*, **384**, 980–991.
57. Hsu,H.L., Gilley,D., Galande,S.A., Hande,M.P., Allen,B., Kim,S.H., Li,G.C., Campisi,J., Kohwi-Shigematsu,T. and Chen,D.J. (2000) Ku acts in a unique way at the mammalian telomere to prevent end joining. *Genes Dev.*, **14**, 2807–2812.
58. Ribes-Zamora,A., Indiviglio,S.M., Mihalek,I., Williams,C.L. and Bertuch,A.A. (2013) TRF2 interaction with Ku heterotetramerization interface gives insight into c-NHEJ prevention at human telomeres. *Cell Rep.*, **5**, 194–206.
59. Xin,H., Liu,D., Wan,M., Safari,A., Kim,H., Sun,W., O'Connor,M.S. and Songyang,Z. (2007) TPP1 is a homologue of ciliate TEBP-β and interacts with POT1 to recruit telomerase. *Nature*, **445**, 559–562.
60. Wang,F., Podell,E.R., Zaug,A.J., Yang,Y., Baciu,P., Cech,T.R. and Lei,M. (2007) The POT1-TPP1 telomere complex is a telomerase processivity factor. *Nature*, **445**, 506–510.
61. Zhong,F.L., Batista,L.F., Freund,A., Pech,M.F., Venteicher,A.S. and Artandi,S.E. (2012) TPP1 OB-fold domain controls telomere maintenance by recruiting telomerase to chromosome ends. *Cell*, **150**, 481–494.
62. Schmidt,J.C., Zaug,A.J. and Cech,T.R. (2016) Live cell imaging reveals the dynamics of telomerase recruitment to telomeres. *Cell*, **166**, 1188–1197.
63. García-Cao,M., O'Sullivan,R., Peters,A.H., Jenuwein,T. and Blasco,M.A. (2004) Epigenetic regulation of telomere length in mammalian cells by the Suv39h1 and Suv39h2 histone methyltransferases. *Nat. Genet.*, **36**, 94–99.
64. Liu,Y., Maekawa,T., Yoshida,K., Furuse,T., Kaneda,H., Wakana,S. and Ishii,S. (2016) ATF7 ablation prevents diet-induced obesity and insulin resistance. *Biochem. Biophys. Res. Commun.*, **478**, 696–702.
65. Brennecke,J., Aravin,A.A., Stark,A., Dus,M., Kellis,M., Sachidanandam,R. and Hannon,G.J. (2007) Discrete small RNA-generating loci as master regulators of transposon activity in *Drosophila*. *Cell*, **128**, 1089–1103.
66 Hackett,J.A., Feldser,D.M. and Greider,C.W. (2001) Telomere dysfunction increases mutation rates and genomic instability. *Cell*, **106**, 275–286.
67. Charles,S.T. and Carstensen,L.L. (2010) Social and emotional aging. *Annu. Rev. Psychol.*, **61**, 383–409.
68. Herrera,E., Samper,E. and Blasco,M.A. (1999) Telomere shortening in $mTR^{-/-}$ embryos is associated with failure to close the neural tube. *EMBO J.*, **18**, 1172–1181.
69. Schaetzlein,S., Lucas-Hahn,A., Lemme,E., Kues,W.A., Dorsch,M., Manns,M.P., Niemann,H. and Rudolph,K.L. (2004) Telomere length is reset during early mammalian embryogenesis. *Proc. Natl. Acad. Sci. U.S.A.*, **101**, 8034–8038.
70. Liu,L., Bailey,S.M., Okuka,M., Muñoz,P., Li,C., Zhou,L., Wu,C., Czerwiec,E., Sandler,L., Seyfang,A. *et al.* (2007) Telomere lengthening early in development. *Nat. Cell Biol.*, **9**, 1436–1441.